Unclassified

ecurity Classification of this page

REPORT DOCUMENTATION PAGE

a. Report Security Classification: Unclassified		1b. Restrictive Markings	
a. Security Classification Authority		3. Distribution /Availability of Report: Approved for public release; distribution is unlimited.	
b. Declassification/Downgrading Schedule			
Performing Organization Report Number(s)		5. Monitoring Organization Report Number(s)	
a. Name of Performing Organization: Naval Postgraduate School	6b. Office Symbol (*If Applicable*): PH/Hf	7a. Name of Monitoring Organization: Naval Postgraduate School	
c. Address (*city, state, and ZIP code*): Monterey, CA 93943-5000		7b. Address (*city, state, and ZIP code*): Monterey, CA 93943-5000	
a. Name of Funding/Sponsoring Organization	8b. Office Symbol (*If Applicable*)	9. Procurement Instrument Identification Number	
c. Address (*city, state, and ZIP code*)		10. Source of Funding Numbers: Program Element Number / Project No / Task No / Work Unit Accession No	

1. Title (*Include Security Classification*) Investigation of the Physical Characteristics of a Mass Element Resonator

2. Personal Author(s): Grant, Larry A.

3a. Type of Report	13b. Time Covered	14. Date of Report (*year, month,day*)	15 Page Count
Master's Thesis	From Jul 89 To Mar 92	March 1992	76

6. Supplementary Notation: The views expressed in this thesis are those of the author and do not reflect the official policy or position of the Department of Defense or the U.S. Government.

17. Cosati Codes			18. Subject Terms (*continue on reverse if necessary and identify by block number*)
Field	Group	Subgroup	Resonators

19. Abstract (*continue on reverse if necessary and identify by block number*): This thesis investigates the characteristics of an acoustic resonator with a passive mass element. The mass element is substituted as an impedance matched replacement for a section of gas-filled half wavelength resonator tube. The mass element consists of a disk bonded to a Servometer electroformed single convolution nickel bellows. The bellows can be modelled as a circular plate with a spring supported boundary placed in the acoustic center of a resonator between two equivalent gas springs driven by a loudspeaker. Loading changes were used to characterize the bellows' motional response to different drive conditions for the frequency range near the first resonance of the system. The response of the system was highly nonlinear for nearly all the configurations despite minimal loudspeaker drive levels. The nonlinear response was a consequence of the coincidence of the resonant frequencies for several modes of the bellows, particularly two prominent modes -- an expected piston-like mode, and an unexpected rocking mode. Attempts were made with varying success to achieve high amplitudes for the piston mode, which is important for its use in a new generation Thermoacoustic Refrigerator. The new refrigerator design will utilize the mass element to reduce those acoustic losses that are a parasitic heat load on the cold end of the refrigerator, as well as make the resonator more compact.

20. Distribution/Availability of Abstract	21. Abstract Security Classification	
[X] unclassified/unlimited [ ] same as report [ ] DTIC users	Unclassified	
22a. Name of Responsible Individual: T. Hofler	22b. Telephone (*Include Area code*): (408) 646-2420	22c. Office Symbol: PH/Hf

DD FORM 1473, JUN 86 Previous editions are obsolete. S/N 0102-LF-014-6603

security classification of this page: Unclassified

Approved for public release; distribution is unlimited.

An Investigation of the Physical Characteristics of a Mass Element Resonator.

by

Larry Allan Grant
Lieutenant , United States Navy
B.A., University of California, 1982

Submitted in partial fulfillment of the requirements for
the degree of

MASTER OF SCIENCE IN SYSTEMS TECHNOLOGY

from the

NAVAL POSTGRADUATE SCHOOL
March 1992

ABSTRACT

This thesis investigates the characteristics of an acoustic resonator with a passive mass element. The mass element is substituted as an impedance matched replacement for a section of gas-filled half wavelength resonator tube. The mass element consists of a disk bonded to a Servometer electro-formed single convolution nickel bellows. The bellows can be modelled as a circular plate with a spring supported boundary placed in the acoustic center of a resonator between two equivalent gas springs driven by a loudspeaker. Loading changes were used to characterize the bellows' motional response to different drive conditions for the frequency range near the first resonance of the system. The response of the system was highly nonlinear for nearly all the configurations despite minimal loudspeaker drive levels. The nonlinear response was a consequence of the coincidence of the resonant frequencies for several modes of the bellows, particularly two prominent modes -- an expected piston-like mode, and an unexpected rocking mode. Attempts were made with varying success to achieve high amplitudes for the piston mode, which is important for its use in a new generation Thermoacoustic Refrigerator. The new refrigerator design will utilize the mass element to reduce those acoustic losses that are a parasitic heat load on the cold end of the refrigerator, as well as make the resonator more compact.

C.1

TABLE OF CONTENTS

ACKNOWLEDGMENTS

I would like to thank my thesis advisor, Dr. Tom Hofler, for all his patient assistance with my non-intuitive approach to physics. Additionally, I appreciate all suggestions and hints from Professor Keolian and Jay Adeff. I also appreciate the coffee and comradery of the Spanagel Hall Late Night Physics Group. Effusive thanks to my wife, Coralee, for handling so much while this thesis came together.

I. INTRODUCTION

A. A BRIEF HISTORY OF THERMOACOUSTICS

In January, 1992, a new kind of refrigerator was carried into earth orbit by the Space Shuttle Discovery on STS-42. Designed to operate on thermoacoustic principles rather than the traditional Rankine (or vapor-compression) refrigeration cycle, the new refrigerator is a practical application of a phenomenon noticed by a number of investigators in the past two centuries and examined but not explained by Sondhauss in a paper published in 1850. As Lord Rayleigh states in a reference to Sondhauss' paper in his *Theory of Sound*, when glass blowers blow "a bulb of about 2 cm. in diameter ... at the end of a somewhat narrow tube, 12 or 15 cm. long, a sound is sometimes heard proceeding from the heated glass." [Ref. 1]. Sondhauss was able to show that this sound was not due to any vibration of the glass, but he was unable, Rayleigh notes, to explain the mechanism that did produce the sound. Rayleigh gave a qualitative explanation of the source of the sound, but many years passed before a quantitative understanding was formulated by Rott and his colleagues working from 1969 into the 1980s. [Ref. 2]

Recent work (early 1980s to the present day) by Wheatley, Swift, and Hofler culminated in the construction of the Space Thermoacoustic Refrigerator, STAR, by Hofler, Garrett and a group of graduate students and technicians at the Naval Postgraduate School. The STAR was a direct descendent of the working thermoacoustic refrigerator designed and built by Hofler as his doctoral degree project [Ref. 3]. The design and

construction of the STAR is described in a group of theses written by the graduate students, Harris and Volkert, Byrnes, Susalla, Fitzpatrick, and Adeff, associated with the project [Refs. 4-8]. Reference should be made to these theses for a more in-depth development of the principles of the thermodynamics and the theory of thermoacoustics than will be given here.

Thermoacoustic refrigerator design is elegant and straightforward. In the case of the STAR, Figure 1.1, the acoustic power source of the refrigerator is a modified commercial Harmon-JBL model 245OJ electrodynamic compression loudspeaker. The modifications to the loudspeaker included the substitution of an aluminum reducer cone for the original titanium diaphragm mounted on the voice coil in order to match the diameter of the driven end of the loudspeaker to the bore of the resonator, and the removal of some unnecessary material around the throat of the loudspeaker. [Ref. 9]

The resonator of the STAR bolts directly to the driver housing and consists of three sections. The first section has three subsections. The upper, or "hot", subsection contains the hot heat exchanger and is located closest to the driver. The middle subsection below the hot heat exchanger contains the stack of parallel plates. The third subsection holds the cold heat exchanger and a reducer. The reducer matches the bore of the first section to the bore of the second section, the pipe. The spherical termination is the third section of the resonator.

The two heat exchangers in the STAR upper resonator section are intricately hand fashioned from a series of parallel copper plates. The method of their manufacture is outlined in detail by Adeff [Ref. 10].

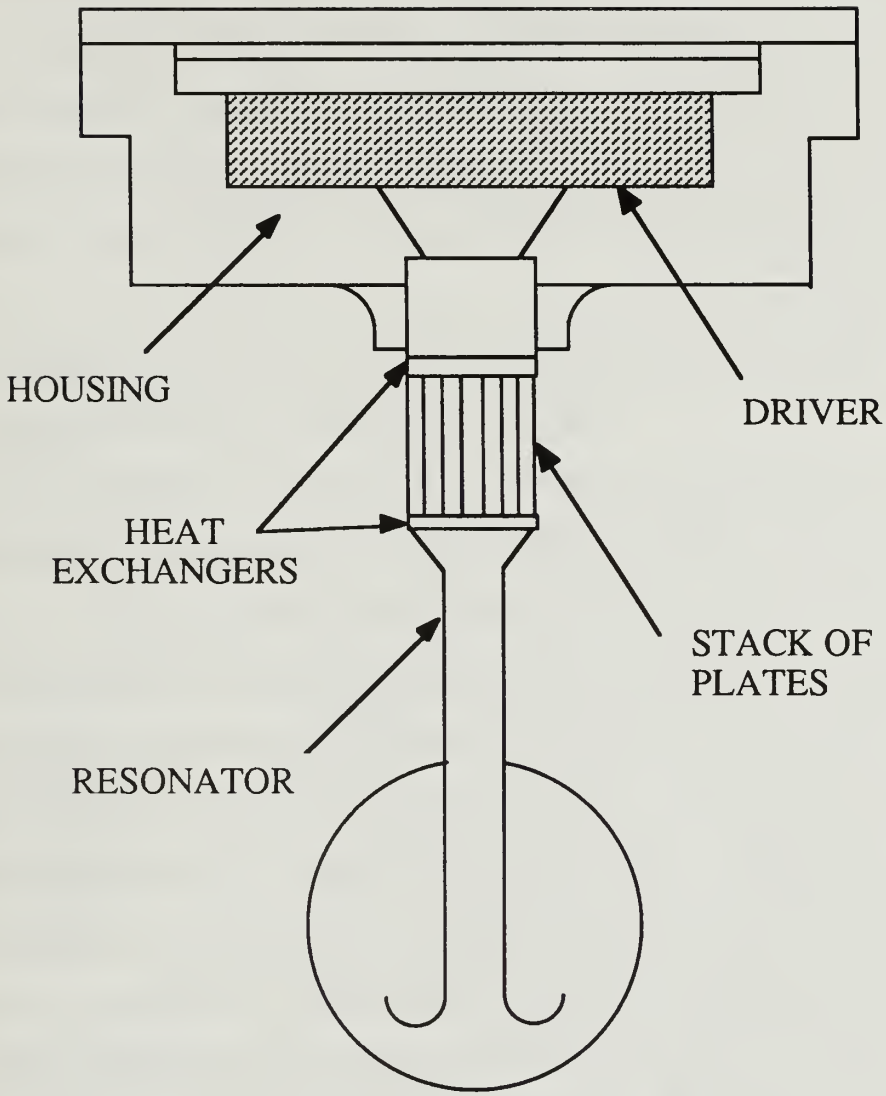

Figure 1.1
The Space Thermoacoustic Refrigerator
STAR

Located between the two heat exchangers is the stack of parallel plates, or stack, for short, the component that provides the medium where the thermoacoustic heat transport process occurs. Designed by Hofler, the current form of the stack is a spiral wound roll of polyester film separated by spacers of monofilament fishing line. Stack manufacture is also covered in detail by Adeff [Ref. 11].

Given the crucial role played by the stack in the thermoacoustic process, a short qualitative discussion will be given of the heat transfer process. A more detailed treatment can be found in a number of the sources, several of which are listed as references, in particular References 2, 3, 12, and 13. Also, any of the theses listed provide a good understanding of the process. In its simplest form, the transfer of heat in a thermoacoustic refrigerator, or TAR, requires the presence of two thermal mediums in the resonator. A plate in the acoustic field is one medium and the gas in the resonator is the other. The presence of the plate allows an irreversible heat flow to take place along the plate as the gas oscillates near the plate surface under the influence of the acoustic driver.

A description of the thermoacoustic process traces the motion of a parcel of gas located along some arbitrary initial position near the surface of the plate. The gas parcel will be displaced to the right, for example, in the first half-cycle of the standing pressure wave in the resonator and simultaneously compressed. (The distance from the parcel to the plate and the amount of time they spend in company are important, but ignored, variables in this discussion. Suffice it to say that the distance to the plate must be on the order of a distance called the thermal penetration depth, and

time sufficient for the process to occur must pass with the parcel in each position.) As the gas parcel is compressed, its temperature increases, and its displacement brings it near a 'new' section of plate which has a lower temperature than the gas parcel. Before the leftward-going component of the standing pressure wave can return the parcel to its initial position, it lingers long enough, and near enough, to the plate to transfer heat to the plate, lowering its own temperature substantially, and raising the temperature of the plate in that locality slightly.

When the parcel expands and returns to its original position during the second half-cycle, it now has, by virtue of its expansion and leftward translation, a temperature that is lower than the temperature of the plate in that 'old' location and another heat transfer takes place, this time from the plate to the gas parcel. Once again the parcel journeys back to the 'new' section of the plate with the rightward-going half-cycle of the standing pressure wave, and when it arrives, it deposits a little more heat to the plate. The heat transferred on its previous trip, in the mean time, has been collected by another gas parcel initially located a little further down the plate, and that heat has been transported down the plate in a bucket brigade fashion, one step further for each pressure cycle. Wheatley says of this process that "effectively, there are many elementary 'engines' in series." [Ref. 14]

The thermoacoustic refrigerator built by Hofler multiplies the effect of these many little engines into a large scale process for heat transference. To make the process more efficient and possibly to allow it to reach cryogenic temperatures is a goal toward which the current thesis is one

step. To take this step requires an understanding of the significance of the resonator to thermoacoustic heat engines and of the loss mechanisms associated with the resonator. This understanding, then, can be applied to controlling losses that occur in the resonator.

B. THE SIGNIFICANCE OF THE RESONATOR IN THERMOACOUSTIC HEAT ENGINE DESIGNS

It is important to understand the significance of the resonator prior to taking an in-depth look at the theory. Therefore, this section will take a brief look at the evolutionary history of the resonator and the changes in refrigerator efficiency that accompanied each step in the evolution to the present resonator. In addition, a few other ways in which the resonator affects the overall efficiency of the TAR will be briefly examined.

All four of the examples of resonator geometry were examined by Hofler in his dissertation and the discussion here will follow his example. The physical changes that occurred in the resonator during its evolution into the current STAR resonator can be seen in Figure 1.2. In (a), the arrangement of the refrigerator has the driver located on the left side of the drawing with the resonator on the right. The stack is located in the far right end of the resonator. This arrangement places the stack in the optimum position with respect to the standing pressure wave in the resonator. The stack, in order to function, depends on the continuous pressure change that is responsible for the temperature oscillation and on the simultaneous displacement oscillation that is responsible for transporting the gas parcels. [Ref. 15]

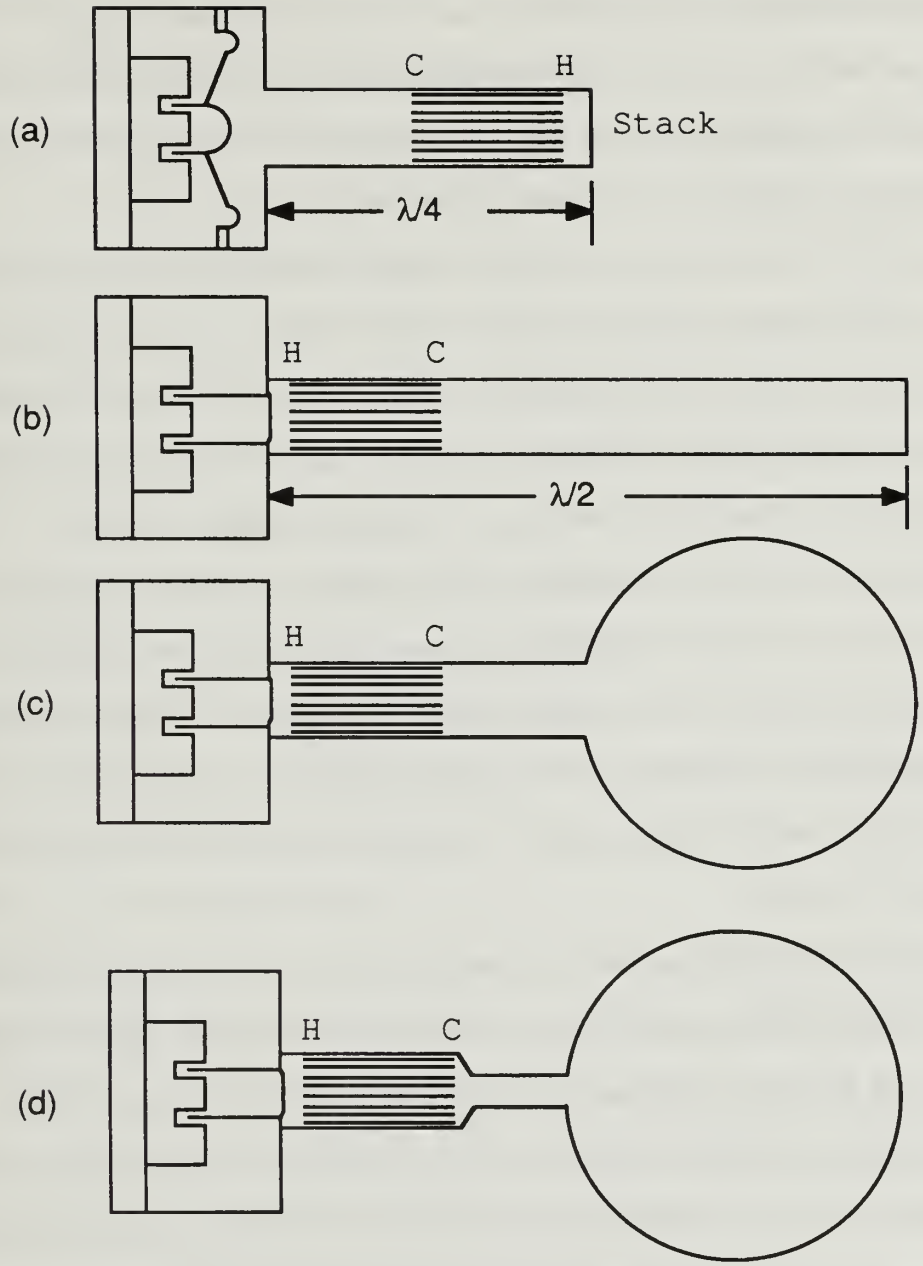

Figure 1.2
Resonator Evolution

The two effects require that the stack not be collocated with either a pressure node nor with a velocity node. The best position is half way between the two. This, as Hofler says, is the position of maximum heat flow. [Ref. 16] For efficiency reasons, the stack is usually placed closer to the pressure antinode than the velocity antinode.

The difficulties with resonator (a) center primarily on the relative position of the driver and the cold end of the stack. In this configuration, the driver not only provides the power required for the thermoacoustic effect; it also transfers heat to the cold end of the stack (via acoustically stimulated convection) and constitutes a nuisance heat load itself.

This problem can be overcome by changing the relative positions of the ends of the stack as is shown in resonator (b). In this resonator, the stack has been moved closer to the driver. The stack must still lie at a position that is one-eighth of one wavelength or less from the velocity node, however, which requires the resonator to be lengthened to one-half wavelength overall.

Now, the driver is located next to the hot end of the stack and is no longer a direct load on the cold end of the stack. This fix does not come without cost, however. The increase in length of the resonator that is required to insure that the stack remains in an optimum position, causes increased viscous and thermal heat losses, since both these quantities are proportional to the surface area. Hofler found that the dissipative losses from a straight, one-half wavelength rigid end resonator were unacceptably high due to this increased length.

The way to avoid this problem is shown in (c), where a spherical termination has been added to a one-quarter wavelength long resonator. The important point to remember is that the thermoacoustic effect depends on the position of the stack with respect to the velocity and pressure nodes and not on resonator length or on a rigid termination. As Kinsler shows, the pressure amplitude of the reflected wave from a pipe with an open end is nearly equal to the amplitude of the incident wave and most of the power in a sound field is confined in an open ended pipe with very little power transmitted out the open end, so a rigid ended pipe is not a requirement [Ref. 17]. The replacement of half of (a) with the sphere in (c) shortens the resonator to one-quarter wavelength which has the effect of once again reducing viscous and thermal losses. By attaching the sphere to the end of the resonator, Hofler found he could reduce the acoustic losses in the cold end of the resonator by more than a factor of two since the cold length of the tube in (b) is about three-eighths of a wavelength long compared to one-eighth of a wavelength in (c).*

In addition, in Figure 1.2 (d), the cross-section of the now shorter one-quarter wavelength resonator was decreased, which reduced the losses in the cold portion of the resonator further by decreasing the length and the surface area of the pipe. The increase in gas velocity that accompanied this change did cause larger frictional losses per unit area, however, this increase was more than offset by the reduction in surface area. A few other, smaller, changes were also incorporated into the STAR resonator

---

* The addition of the sphere is a necessary condition to approximating an open termination since the system is normally pressurized to ten bar.

but the most significant changes to arrive at the final configuration were these. [Ref. 18]

In addition to the ways mentioned above, the resonator also affects the efficiency of the Thermoacoustic Refrigerator by modifying the sound field and interacting with the components in the sound field. A few more examples will illustrate some of these contributions of the resonator to the thermoacoustic refrigeration process according to its effect on the sound field and its effect on the driver.

The effect that the resonator has on the sound field is an important one. As has been mentioned, the thermoacoustic effect depends on the movement and corresponding compression and rarefaction of the gas through which the sound field passes. Driving a gas-filled pipe on resonance creates and confines a very strong sound field with rapid, and, if desired, large acoustic pressure variations. These variations in pressure create correspondingly large changes in temperature which directly affects the amount of heat transported. This is particularly true since the gas-tight resonator is pressurized.

The resonator also provides an acoustic environment whereby large acoustic pressures and velocities can be created from relatively small oscillations of the driver piston. At resonance, however, the position of the driver closely resembles a velocity node and exhibits very little movement. This is true whether the resonator is a rigid ended pipe or an open ended pipe. The small motion of the driver piston allows the use of a flexible diaphragm instead of a normal piston and piston rings (i.e., sliding seals).

So the resonator is an important factor in simplifying the driver hardware and increasing reliability.

In this section of the paper, the development of the resonator and its importance to thermoacoustic efficiency has been stressed. It should be obvious that proper design of the resonator can substantially reduce thermal and viscous losses. The profit that comes from reducing the generation of heat in or the flow of heat into the cold portion of the resonator is substantial and this has been the primary motivation behind resonator design to this point. Any extra heat load on the cold portion of the cryocooler, not only decreases the temperature span of the engine, but is also multiplied by an order of magnitude or more by the time it is rejected at the room temperature heat exchanger.

The subject of this thesis developed from a desire to reduce the losses even further. Given the large effort required to remove even a small amount of heat from the cryogenically cooled end of the refrigerator, there is a proportional reward to any successful effort to prevent heat from entering the refrigerator in the first place. Changing the size and/or the shape of the resonator has shown that is can reduce the heating of the cold end by reducing thermal/viscous dissipation mechanisms and by reducing the amount of external surface area exposed to the warm surroundings which add heat to the cold resonator.

The substitution of a mass element for a portion of the gas-filled resonator is seen as a way to achieve greater efficiency by reducing the nuisance heat load. The mass element resonator will have a much smaller surface area than an equivalent straight pipe one-half wavelength resonator,

realizing approximately a 4 to 1 reduction in surface area, which translates into reduced thermal/viscous losses and less exposed surface area and, it is hoped, an increase in efficiency.

C. SCOPE OF THE THESIS

This thesis describes one of the continuing modifications now begun in order to make a cryocooler version of the Thermoacoustic Refrigerator, TAR, that can achieve much colder temperatures, possibly approaching liquid nitrogen temperatures. The modification that is the subject of this thesis is the substitution of a solid mass-spring element as an impedance matched replacement for a section of the gas-filled resonator tube. In particular, the physical characteristics quantifying the behavior of the element, a Servometer electroformed single convolution nickel bellows, will be explored.

Chapter II begins with a look at resonator theory from the starting point of the rigid-rigid pipe. The mass element is introduced as a modification to previous resonators, and a theory is presented for the substitution of a mass element for a section of gas filled resonator tube. Finally, the proposed mass element, the Servometer bellows, will be scrutinized in an attempt to describe its physical characteristics. Following the description of the bellows' characteristics, the design and construction of the resonator used for the experiments in this thesis will be described in Chapter III, along with the bench tests conducted prior to mounting the resonator to the driver.

Chapter IV will present the hopes and dreams of the experimenters in a section on experimental intentions. The second section of Chapter IV

addresses the experimental setup and data collection techniques. Finally, the third section tells how reality intruded into our hopes and dreams. As the project unfolded, the appearance of nonlinearities in the vibration of the bellows required it to be modified in various ways to control the undesirable motions of the bellows in the hope of making it conform to the motion of a planar piston resonating at the same frequency and with the same impedance as the section of replaced gas.

Chapter V constitutes the final chapter of this thesis, and offers a few suggestions and conclusions, but since this thesis constitutes one small step at the beginning of a series of investigations that should ultimately result in a new generation of thermoacoustic refrigerators, the finality of any conclusions or recommendations depends directly on the work to follow. It examines only one part of the next generation refrigerator, the addition of a mass element in the resonator. Ultimately, a great deal of work will be required before a new refrigerator can be constructed, and it is to be hoped that this thesis will provided some useful insight for future authors.

II. THE ACOUSTIC RESONATOR

A. RESONATOR THEORY AND MASS SUBSTITUTION

1. Simple Resonator Theory

The resonator theory presented here uses choices related to system design made for other refrigerator resonators as a starting point for the design of the mass element resonator. The operating frequency, pressure, and gas medium in the resonator were each selected to optimize certain criteria in the systems that preceded the present resonator. These particular choices were made to improve general refrigerator efficiency with respect to the cooling achieved in terms of power expended which is a major concern in any refrigeration system.

The primary motivation for modifying the resonator comes directly from a desire to increase refrigerator efficiency by reducing the heat load on the cold end of the resonator by resonator surface area reduction. Even a small reduction in the heat load at the cold end of the resonator can allow much colder temperatures to be achieved, and provides savings of a much greater magnitude in terms of the amount of work required to operate the system to a given temperature.

To allow comparison of the mass element resonator to a simple resonator whose characteristics can be determined easily, the theoretical portion of this paper begins with a look at a simple straight pipe resonator as shown in Figure 2.1.a. Figure 2.1.b shows the modification of the straight pipe resonator by the addition of a mass element. The mass

(a)

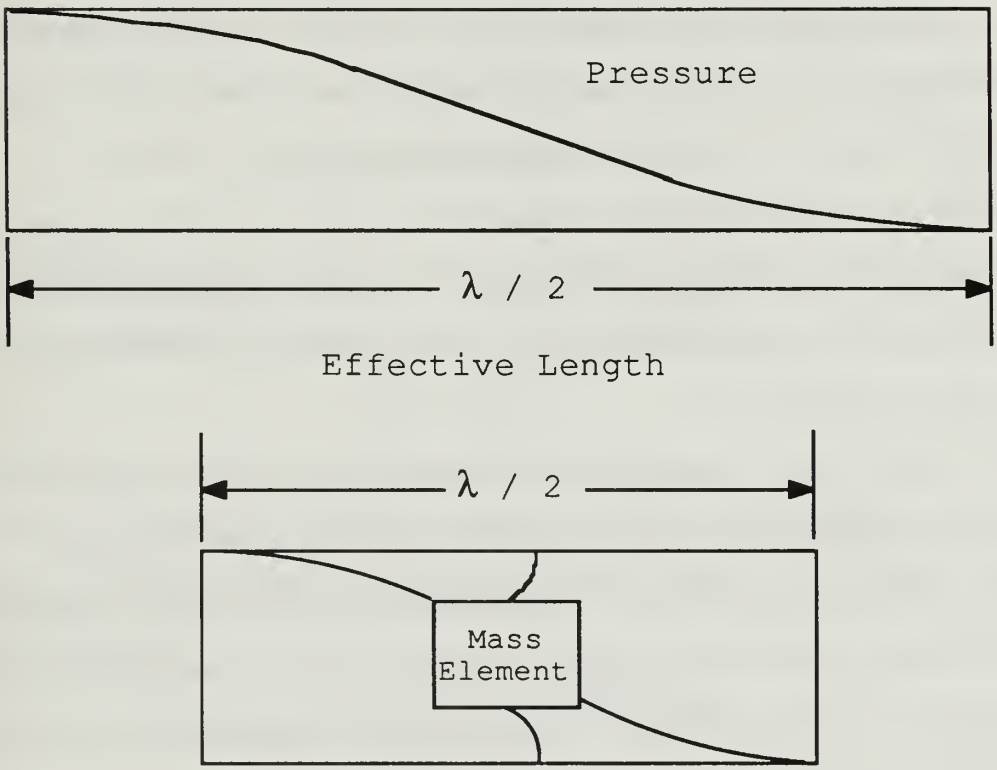

(b)

Figure 2.1.
Schematic Representation Of The Insertion
Of A Mass Element Into A Resonator
With The Pressure Profile Shown

element is inserted in the resonator as an acoustic replacement for a section of the pipe resonator. This replacement results in a reduction of the surface area of the mass element resonator when compared to the straight pipe resonator which contributes to increased efficiency.

The simple straight pipe resonator chosen as the theoretical basis of the mass element resonator has rigid-rigid terminations and is one-half wavelength long to simplify the theoretical description. This is a reasonably good approximation to a driven-rigid pipe at the resonance where the system is designed to operate. At resonance the displacement and velocity of the driver diaphragm is very small, and the driver end looks like a velocity node.

The acoustic impedance of the cold portion of the resonator in a TAR at the location of the cold end of the stack has a predominantly reactive value that is mass-like. An expression for this acoustic impedance will be found, and then the second expression will be found for the acoustic impedance of the mass element. Equating these two expressions will allow a determination of the amount of mass needed to replace a given length of resonator. The expression for the impedance of the straight pipe resonator will be found from the method outlined in Kinsler and Frey [Ref. 19].

For the theoretical development, the operating frequency was chosen to be 500 Hz, the mean pressure in the resonator to be 10 bar, and helium as the gas medium in keeping with previous refrigerator design. These parameters allow the dimensions of the theoretical straight pipe resonator to be fixed according to the physical characteristics of an internal pressure standing wave in the resonator. In the actual experiment, a range

of frequencies and mean pressures including these were used to determine the characteristics of the assembled mass element resonator under different operating conditions.

The radius of the resonator tubing for all resonators in this experiment is 1.64 cm., which is much less than the wavelength of the standing wave, so that it may be assumed that only plane waves of the form

$$p = Ae^{j(\omega t+kx)} + Be^{j(\omega t-kx)} \tag{2.1}$$

exist in the straight resonator. A simplified force equation, the one-dimensional, linear, inviscid form of Euler's equation,

$$\rho_o \frac{\partial u}{\partial t} \approx - \frac{\partial p}{\partial x} \tag{2.2}$$

is used to give an expression for the particle velocity in the pipe. Solving (2.2) for u and substituting into (2.1) gives the following expression for particle velocity

$$u = - \frac{1}{\rho_o c}\left[Ae^{j(\omega t+kx)} - Be^{j(\omega t-kx)}\right]. \tag{2.3}$$

Combination of (2.1) and (2.3), and using the fact that the volume velocity, U, is equal to the particle velocity, u, multiplied by the effective cross-sectional area of the resonator, S_o, gives the following expression for the acoustic impedance, $Z_{ac(pipe)}$, of the straight pipe

$$Z_{ac(pipe)} = \frac{p}{uS_o} = - \frac{\rho_o c \left[Ae^{j(\omega t+kx)} + Be^{j(\omega t-kx)}\right]}{S_o \left[Ae^{j(\omega t+kx)} - Be^{j(\omega t-kx)}\right]}. \tag{2.4}$$

When it is evaluated at x=0 and at $x=X_m$, where X_m is the distance from the rigid termination to the mass element, (2.4) gives two equations for $Z_{ac(pipe)}$ that can be combined to eliminate the constants A and B. Eliminating A and B gives $Z_{ac(pipe)}(x=X_m)$ in terms of $Z_{ac(pipe)}(x=0)$. If it is assumed that the impedance at the rigid end at x=0 is infinite, then the input impedance of the straight pipe is given by

$$Z_{ac(pipe)}\,(x = X_m) = j\frac{\rho_o c}{S_o}\cot(kX_m) \tag{2.5}$$

or, in terms of the mean pressure in the resonator, where the speed of sound is given by

$$c = \sqrt{\frac{\gamma p_m}{\rho_o}} \tag{2.6}$$

$Z_{ac(pipe)}$ becomes

$$Z_{ac(pipe)}\,(x = X_m) = j\frac{\gamma p_m}{cS_o}\cot(kX_m). \tag{2.7}$$

This expression gives the acoustic impedance of the straight pipe resonator in terms of the mean pressure in the resonator, p_m, the ratio of specific heats for helium, γ, the cross-sectional area of the pipe, S_o, and the speed of sound in helium, c, as a function of the distance, X_m, from the rigid termination. The next step in substituting a mass for some portion of the pipe resonator with this impedance is to find the acoustic impedance of the mass element.

2. Mass Element Substitution

To find the equivalent acoustic impedance of a mass so that it may be substituted for a section of the pipe resonator, a method suggested by Hofler will be used. The assumption is made that the mass and its support

can be modeled as a simple harmonic oscillator. The mechanical impedance of a simple harmonic oscillator can be written

$$Z_{mech(mass)} = R + jX \tag{2.8}$$

where R is the mechanical resistance and X is the mechanical reactance.

The reactance, X, for a simple harmonic oscillator is given by

$$X_{mech(mass)} = \left(\omega m - \frac{s}{\omega}\right) \tag{2.9}$$

where the frequency is z, the effective mass of the mass element is m, and the spring constant is s. Since the mechanical resistance, R, is very small and dominated by losses elsewhere in the system, it will be neglected, and the expression for the mechanical impedance becomes

$$Z_{mech(mass)} = j\left(\omega m - \frac{s}{\omega}\right). \tag{2.10}$$

The relationship between the mechanical impedance of the mass and the acoustic impedance of the mass is given by

$$Z_{mech} = Z_{ac} S_m^2 \tag{2.11}$$

where S_m is the effective cross section area of the mass (actually determined by the effective area of the bellows). Dividing (2.10) by the squared effective area of the mass gives an equation for the acoustic impedance of the mass which can then be related to the acoustic impedance of the straight pipe resonator.

The relationship between the acoustic impedance of the mass and the acoustic impedance of the pipe is established by referring to the definition of mechanical impedance. Mechanical impedance is defined as

the ratio of the driving force to the velocity at the point of application of the force, or

$$Z_{mech} = \frac{f}{u}. \tag{2.12}$$

Recognizing that $f = pS_m$, where p is pressure, and then dividing (2.12) by S_m^2, as in Equation (2.11) gives the following expression for acoustic impedance

$$Z_{ac} = \frac{p}{uS_m}. \tag{2.13}$$

This expression applies to the mass element, but it cannot be related directly to the acoustic impedance for a pipe until we have a clear understanding of what is meant by the pressure, p, on the mass element.

The pressure, p, can be seen from Figure 2.2 to refer to the pressure difference across a mass element located in a short resonator. The mass in this resonator has been displaced from its equilibrium position, and it can be seen that the total pressure on the mass is equal to the difference in the pressures on either side of the mass element, or

$$p = p^+ - p^-. \tag{2.14}$$

If the two volumes on either side of the mass were the same before displacement of the mass, symmetry of the volume velocity implies that $U^+(Xm)=U^-(Xm)=u$, and anti-symmetry of pressure and acoustic impedance implies that $p^+ = - p^-$ and $p = 2 p^+$ and that $Z^+(Xm)=Z^-(Xm)$. The acoustic impedance of the mass element becomes

$$Z_{ac(mass)} = \frac{2p^+}{uS_m}. \tag{2.15}$$

But the acoustic impedance of the pipe is just p^+/uS_m so that the relationship of acoustic impedances for the mass and pipe is

$$Z_{ac(mass)} = 2Z_{ac(pipe)}. \tag{2.16}$$

Substitution of Equations (2.7), (2.10), and (2.11) into (2.16) and solving for the mass, m, gives the desired relationship between the mass of the mass element and a resonator of length L. This is Equation (2.17):

$$m = 2\frac{\gamma p_m S_m^2}{\omega c S_o}\cot(kX_m) + \frac{s}{\omega^2}. \tag{2.17}$$

This equation will be used to find the mass needed to build a mass element resonator equivalent to a straight pipe resonator with the desired resonant frequency.

B. THE MASS ELEMENT

Prior to actually constructing the mass element resonator and conducting any experimental runs, it was hoped, particularly by the author, that this would be a straightforward project with no extraordinary turnings or twistings. As it has turned out, this has not been the case and, in large part, this can be attributed directly to the qualities of the bellows chosen for suspension for the mass element in this experiment.

The suspension used was a 1.5 inch O.D. Servometer electroformed single convolution nickel bellows. Given the time constraints on the author, this bellows offered one very important characteristic, shared with mountain peaks, that could not be overlooked: It Was There. A custom 2.25 in. bellows had been designed and placed on order five months prior

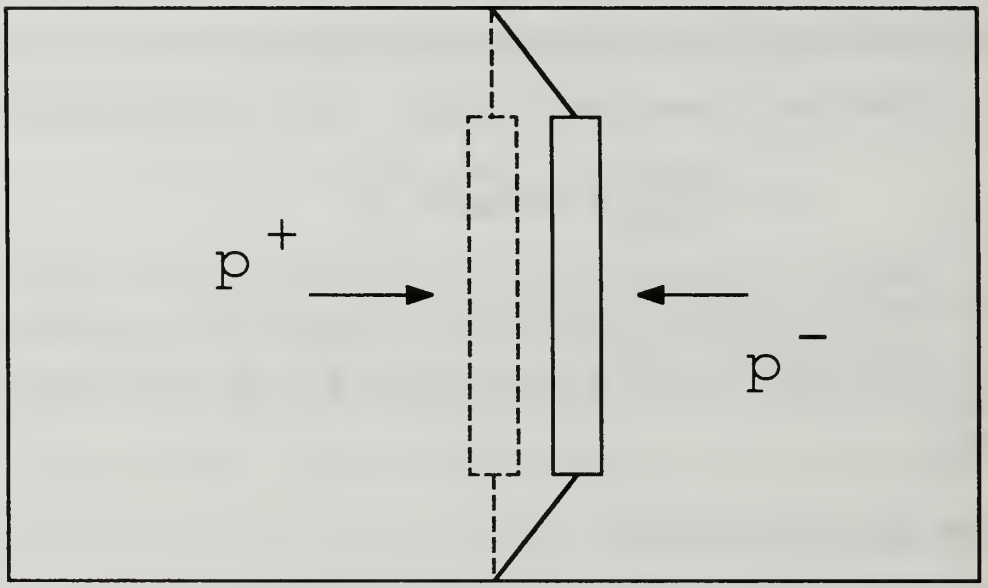

Figure 2.2.
Schematic Of Pressure On
A Mass Element In A Resonator

to the design and construction of the resonator discussed here, but was not available for these experiments.

As will be explained in a later section, the behavior exhibited by this bellows was more complicated than expected. Instead of a clean linear response to a driving signal, the bellow's motional response was very nonlinear to modest drive levels and above, over a substantial frequency range. It is hoped that the results of these experiments will contribute clues that will help reduce or eliminate the nonlinearities so that construction of the next version resonator can proceed.

The general appearance of the Servometer bellows is shown in Figure 2.3. The technical specifications can be found in the manufacturer's data sheet included in Harris and Volkert. The bellows is formed by an electroplating process that deposits nickel onto an aluminum mandrel. The plating process proceeds until the thickness of metal needed for a particular application is reached. The bellows used in the experiments of this thesis has a uniform wall thickness of about 0.0025 inches. The thickness is probably not uniform for all surfaces, however.

Essentially, the shape of the bellows is that of a short hollow cylinder with one end open and the other end closed. Various convolutions added to the side wall to change the bellows spring characteristics and modify the shape from that of a simple cylinder.

Once the bellows' wall has reached the desired thickness, the aluminum mandrel is removed by a wasting process. The resulting bellows can be thought of as a circular plate of nickel supported around its perimeter by a continuous nickel spring that is in turn fastened to the collar

around the base of the bellows. This last feature around the base of the bellows allows it to be soldered into place in the resonator.

C. THE MASS ELEMENT RESONATOR MECHANICAL/ ELECTRICAL ANALOGY

A mechanical/electrical analogy was formulated to give the author a better understanding of the response to be expected from the mass element resonator. The mechanical analogy used a simplified image of the bellows as a circular plate supported by springs. The resonator was modeled as a simple harmonic oscillator with additional springs to account for the action of the gas in the volumes above and below the bellows. Resistance terms were also included for the gas but not for the bellows since it was felt that the resistance components of the gas were much greater than the resistance of the bellows. The mechanical model is shown in Figure 2.4.

The components of this analogy represent the components of the mass element resonator. Starting from the left, the rigid termination of the resonator is shown. The two springs in the next section represent the bellows spring and the springiness of the gas trapped in the volume between the bellows and the rigid termination of the resonator. R(gas) is the analog of the various resistance components of the gas in this volume.

The next component is the moving mass of the bellows. To the right of the mass is another gas spring and another dashpot representing the resistance in the volume between the bellows and the driver. Finally, in the position farthest to the right, the driving force of the loudspeaker is represented by a force vector.

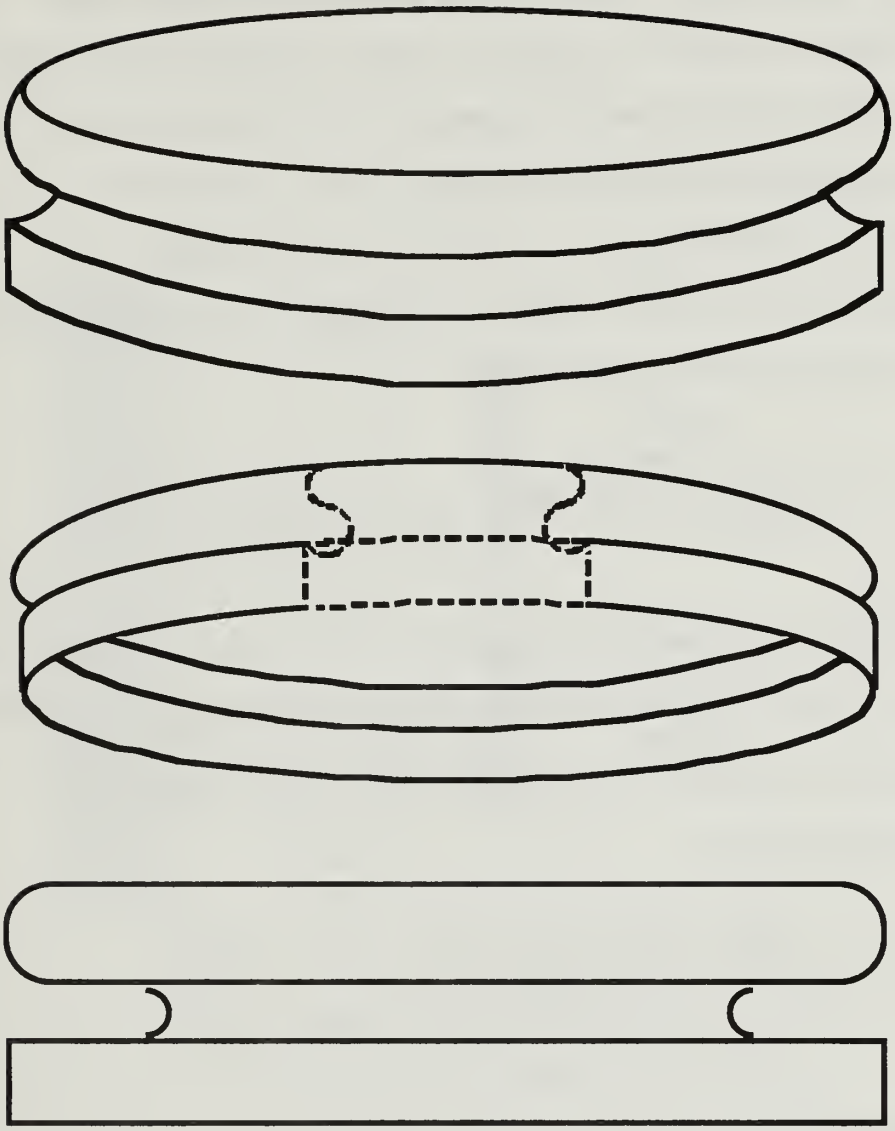

Figure 2.3 The Servometer Bellows

From this mechanical circuit, an electrical equivalent circuit can be drawn and an expression written for the impedance of the circuit. The electrical circuit is shown in Figure 2.5. The components in the electrical circuit are the same components present in the mechanical circuit. In this case, the spring constant of the mechanical circuit is shown as a compliance, C, with the type of compliance in parenthesis.

Using circuit laws and writing an expression for the impedance of this circuit gives the following expression

$$\frac{1}{Z} = \frac{1}{\left(R + \frac{1}{j\omega C_{gas}}\right)} + \frac{1}{\left(R + j\omega M + \frac{1}{j\omega C_{gas}} + \frac{1}{j\omega C_{bellows}}\right)}. \tag{2.18}$$

In this case, M is the effective moving mass of the mass element, C_{gas} and $C_{bellows}$ are the compliances given by $1/S_{gas}$ and $1/S_{bellows}$, respectively. Rewriting this equation to give the magnitude of the impedance in mechanical terms gives

$$|Z| = \sqrt{\frac{2R^3 + 2RS_{gas}X + RY^2}{(4R^2 + Y^2)} + \frac{R^2Y - S_{gas}X}{(4R^2 + Y^2)}} \tag{2.19}$$

where X and Y are

$$X = M - \frac{S_{gas} + S_{bellows}}{\omega^2}$$

$$Y = \omega M - \frac{2S_{gas} + S_{bellows}}{\omega}. \tag{2.20}$$

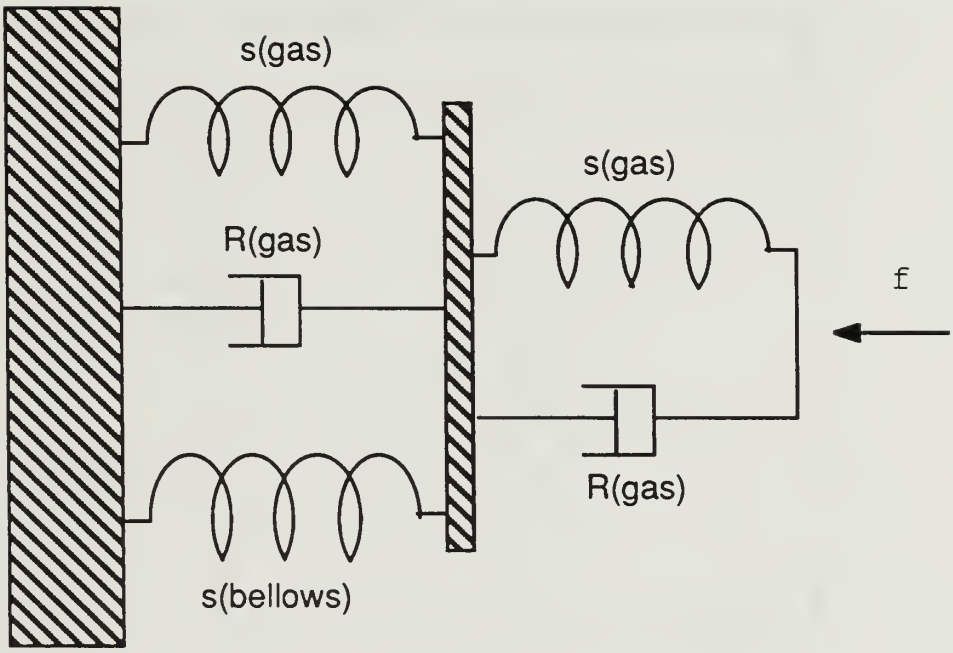

Figure 2.4
The Mass Element Resonator
Mechanical Analogy

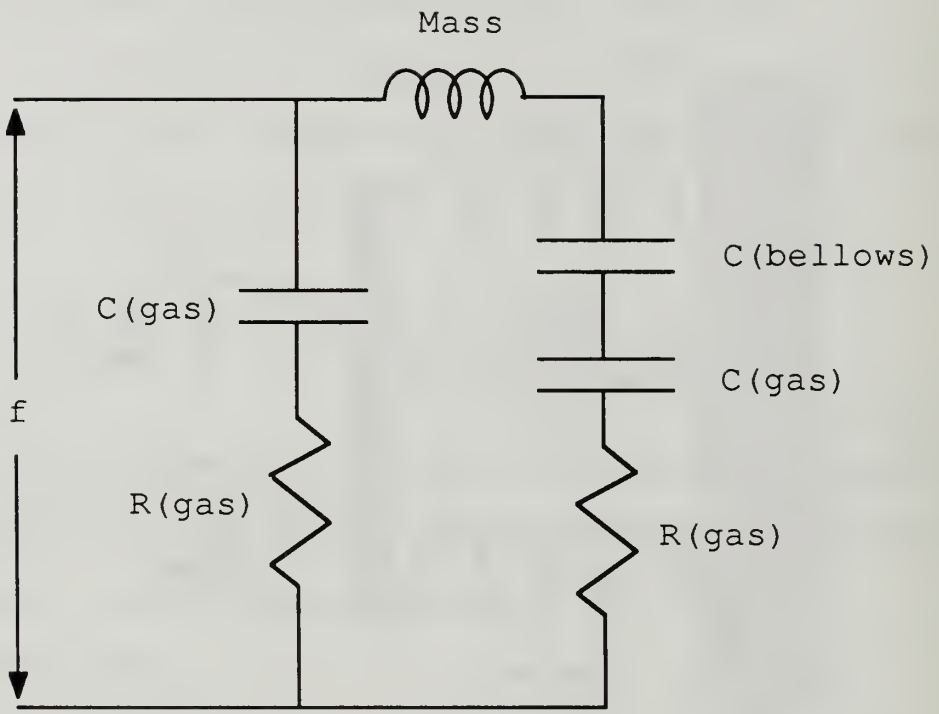

Figure 2.5
The Electrical Equivalent
Circuit

The utility of this expression comes from being able to find the magnitude of the impedance which can then be plotted for comparison against the measured impedances of the mass element resonator which will be the primary variable examined in the experimental portion of the paper. This will be done at the end of Chapter III after the effective moving mass and the spring constant of the bellows have been found. At that time, a value will also be found for the spring constant of the gas springs.

III. DESIGN AND CONSTRUCTION OF A MASS ELEMENT RESONATOR

A. DESIGN AND ASSEMBLY OF THE MASS ELEMENT RESONATOR

The mass element resonator was designed through the combined efforts of Tom Hofler and Jay Adeff. A principal constraint on the design was the need to use the bellows already in hand rather than wait for the new, larger bellows that will be used in later resonators. The current bellows is one and one-half (1.5) in. O.D. and is mounted between two flanges attached to two sections of one and one-quarter (1.25) in. I.D. (nominal) copper pipe. Figure 3.1 shows the final version of the mass element resonator as it was assembled.

For the purposes of the mass element resonator test, the physical dimensions of the resonator were fixed by choosing a stack length of 3.09 in. and a combined length for both heat exchangers of 0.36 in. A distance of 0.75 in. was included to represent the effective real length of the mass element junction and an additional 0.5 in. was included to account for the driver to heat exchanger distance. As a first approximation, the interior physical length of this resonator was 4.69 in. or 11.91 cm. for one side of the resonator.

This length gives a value for kX_m in Equation (2.17) from Chapter II of 0.3654.

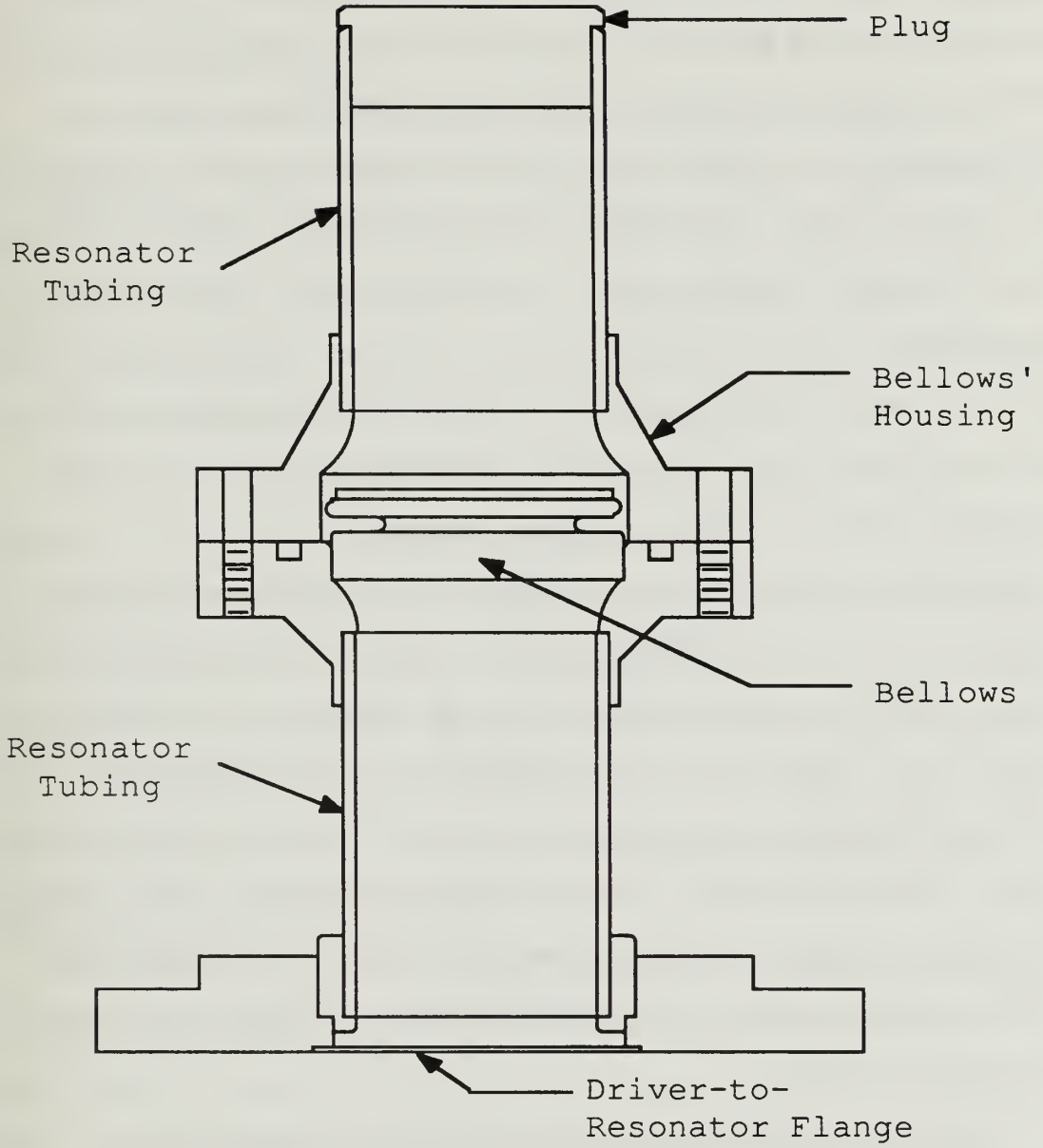

Figure 3.1.
The Mass Element Resonator

$$m = 2\frac{\gamma p_m S_m^2}{\omega c S_o}\cot(kX_m) + \frac{s}{\omega^2}. \qquad (3.1)$$

Assumptions can then be made concerning the other values in the equation to arrive at a figure for the mass. The desired operating resonant frequency was chosen to be 500 Hertz and the speed of sound in helium to be 1024 m/s at 300°K. A operating mean pressure, p_m, of eight bar was picked. The ratio of specific heats, γ, for helium is 5/3. The cross-sectional areas of the mass and the resonator tube are 7.458 cm. and 8.432 cm., respectively. The spring constant of the bellows' spring from the manufacturers data sheet is 3680 N/m. Substitution of these values into (3.1) gives a mass of 1.8 gm. for the mass element.

This value is just about equal to the weight of the bellows which is 1.78 gm. Since it was desirable to be able to vary the mass of the bellows in order to perform the fine tuning of the mass element that was likely to be required, the value for kX_m was decreased to 0.297 and the mean pressure of the system was increased to ten bar. This gives a weight of 2.58 gm. for the total weight of the mass element. Based on this figure and an assumed moving mass of the bellows of 1.46 gm., a net weight margin of 1.12 gm. was available if the figure of 2.58 gm. proved to be too high for the mass element.

The first step in the assembly process was the addition of the additional weight for the mass element which was provided by aluminum disks cut to fit the top of the bellows. Two sizes were made, the larger with a weight of 1.06 gm. and the smaller with a weight of 0.76 gm. For the first series of test runs of the resonator one large disk was epoxied to

the bellows for a combined mass element weight, including epoxy, of 2.93 gm. and a projected moving weight of approximately 2.52 gm., a figure later revised downward.

After the flat exterior rim of the bellows was tinned with a low temperature solder, these disks were attached to the face of the bellows with HYSOL EA 956 epoxy manufactured by Dexter Adhesives and Structural Materials. The epoxy is very strong and fairly insensitive to elevated temperatures. Prior to soldering the bellows to its support flange the bellows was placed in an oven and cured overnight at 40°C.

Use of a low temperature solder to tin the bellows served two purposes. First, even if the epoxy was heat insensitive, it was felt that it was better not to expose it unnecessarily to large temperatures. Second, some modifications to the bellows can be performed more easily with the bellows out of the resonator. By using a low temperature solder for the bellows and higher temperature solder for the other resonator joints, the bellows could be removed without disturbing the other soldered joints which need to remain helium-tight.

The bellows was tinned using the indium solder, Indium Corporation IND #1E, and Kester 817 stainless steel flux. First, a small drop of solder was deposited on the bellows in a position wetted with flux. A drop of solder was then chased around the rim of the bellows with the tip of a soldering iron wetted in flux. The lowest heat setting possible was used. The finished bellows was cleaned with soap and water and rinsed in alcohol to remove any excess flux. As previously mentioned, attachment of the

aluminum disk followed tinning. The bellows was not soldered into the body of the resonator until leak testing had been finished.

The assembly of the other components of the resonator was straightforward and presented no particular difficulty. Kester SN60 solid wire solder was used with Kester 715 copper/brass flux. Parts were cleaned with soap, water and a solvent rinse, then tinned and assembled. Additional solder was added to all solder joints to ensure a helium-tight joint.

B. BENCH TESTS OF THE MASS ELEMENT RESONATOR

1. Leak Testing The Resonator Body

The first bench test of the resonator prior to soldering the bellows into place was the helium leak test. Since the resonator was designed to operate around ten bar in helium, leak testing was necessary to prove it gas-tight. Leak testing was accomplished using an ALCATEL A110TCL leak tester. The resonator was assembled with O-rings in place and placed on the ALCATEL tester. The tester operates by pulling a vacuum on the part and then sampling the gas it removes from the object under test. A stream of helium is played on the part's exterior and if leaks are present some of the gas is sucked into the part. The gas is sent to a mass spectrometer, allowing the tester to detect very small helium leaks. On the resonator the leak rate was found to be about $0.75\text{-}1.5 \times 10^{-8}$ Atm·cm.^{3}/second with an error of $\pm 0.25 \times 10^{-8}$ Atm·cm.^{3}/second. This was an acceptable rate for this resonator. After leak testing was completed, the bellows was soldered into place in the center flange nearest the driver.

2. Bellows Effective Mass And Spring Constant Determination

The two basic assumptions concerning the characteristics of the bellows made prior to construction of the mass element resonator was that the primary oscillatory mode would be a piston-like mode and that the oscillatory response for small amplitude driving forces would be linear. Therefore, it was felt that knowing the effective moving mass of the bellows and the static spring constant was an important first step in getting to know the bellows.

Determination of the effective moving mass and the the spring constant of the bellows was accomplished after the first steps in the assembly process had been completed to insure that the portion of the bellows in motion during the test was the same as during operation of the resonator. This also provided the most secure method of holding the bellows in place during the test.

The relationship of a simple harmonic oscillator's resonant frequency to its mass

$$\omega_o = \sqrt{\frac{s}{m_o}} \tag{3.2}$$

was used to find the effective mass and the spring constant of the bellows. The assumptions made in using this relationship were that the spring constant was indeed a constant and that the damping was so small as to be negligible. The first assumption holds only for infinitesimal displacement amplitudes. The second is a fairly good approximation since, for what turns out to be a small mass, the Q is high, greater than 1500, and the

damped and undamped natural angular frequencies are within 0.1 percent of each other.

The test was conducted by placing the bellows and its support in a vacuum chamber sitting on a shaker table. The vacuum chamber isolated the bellows spring from any effects that might be attributed to trapped or entrained air. The shaker table was driven by a sine wave function generator at very low amplitudes since neither the vacuum chamber nor the bellow's support could be physically fastened to each other or to the shaker table. The mass of the whole system was sufficient so that at the low amplitudes used, only the bellow's face was in relative motion.

Data was taken using a Mechanical Technology, Inc., MTI 1000 Fotonic Sensor. The Fotonic is a non-contacting fiber optic displacement and vibration measurement instrument. It operates by lighting a target area on the surface of the object of interest and measuring the amount of light reflected from the illuminated surface. Displacement or vibration causes a variation in the amount of light received by the fiber optic probe and this variation generates a signal that can be used to determine amount of displacement or frequency of the vibration. In this case, the Fotonic was used as a vibration sensor. The signal from the Fotonic was sent to a Hewlett Packard HP 3561A Dynamic Signal Analyzer for determination of the fundamental resonance of the bellows under various loading conditions.

The experimental procedure was to attach a mass symmetrically to the bellow's face and vibrate the bellows to find the fundamental resonance for the bellows-mass combination. Knowledge of the amount of mass added in each case and its associated resonant frequency allowed the

effective moving mass of the bellows to be determined through the use of Equation (3.2). The moving mass of the bellows, m_o, using a modified version (3.2) of that takes the added mass into account and eliminates s, is given by

$$m_o = \frac{\omega_n^2 \Delta m}{\omega_o^2 - \omega_n^2} \tag{3.3}$$

where ω_n^2 is the resonant frequency when the mass Δm is added to the bellows. Table 2.1 shows the values recorded for each Δm and the associated resonant frequency, ω_n^2, and the computed m_o for each. The average values for m_o and s are included at the bottom of the table.*

TABLE 2.1. BELLOWS MASS AND SPRING CONSTANT

Run	Δ_m	f_o	m_o	s
1	1.1605 g	170.12 Hz	2.0402 g	3657 N/m
2	2.3094 g	144.75 Hz	1.9790 g	3547 N/m
3	4.6194 g	116.80 Hz	1.9842 g	3557 N/m

m_o(mean) = 2.0011 g

s (mean) = 3587 N/m

Having found the effective moving mass and the value of the spring constant for the bellows, a value will be found for the spring

*The values shown for m_o should be decreased by 1.0556 g because at this point an aluminum disk had already been added to the bellow's face in order to provide a rigid mounting plate and in anticipation of the next phase of the experiment.

constant of the gas springs so that the expression given earlier for the magnitude of the impedance can be evaluated.

3. Gas Spring Constant Determination

The gas spring constant can be found by assuming that the volume above and below the bellows is the same. The volume of the resonator, 166.8 cm.^{3}, was found by filling it with water from a burette. The spring constant will be found for one-half of this volume. Adiabatic conditions and uniform pressure in the volume are assumed which gives the following relationship for pressure and volume

$$pV^{\gamma} = \text{CONSTANT} \tag{3.4}$$

where γ is the ratio of specific heats for helium which is 5/3.

Differentiating (3.4) using the product rule and separating the pressure and volume variables gives

$$\frac{dp}{P_m} = -\gamma\frac{dV}{V_m} \tag{3.5}$$

where p_m and V_m are the mean pressure and volume. The numerators dp and dV represent the change in pressure and volume. Force can be written as $f=dp\cdot S_o$, and the displacement as $x=dV/S_o$, which allows Hookes' Law to be solved for the spring constant in terms of pressure, volume, γ, and the cross sectional area of the resonator. This is

$$s = -\frac{f}{x} = -\gamma\frac{p_m S_o^2}{V_m}. \tag{3.6}$$

Using a mean pressure of 10 bar, a volume of 83.4 cm.^{3}, and S_o of $8.432\text{x}10^{-4}$ m.^{2} gives a spring constant for the gas springs of 14208

N/m. This dominates the bellows motion by being about four times greater than the bellows spring constant.

Returning with these values to the expression given at the end of Chapter II for the magnitude of the impedance of the resonator analogy gives the following normalized plot of impedance magnitude versus frequency with resonance at about 630 Hz. It will later be seen that this is a good representation of the impedance magnitude for the resonator at very low drive levels but breaks down rapidly at higher drive levels. Also, the actual resonant frequency is lower than 630 Hz, because the true stiffness of the gas volumes is related to Equation (2.7), which would give a lower value for stiffness than the uniform pressure gas volume model used here.

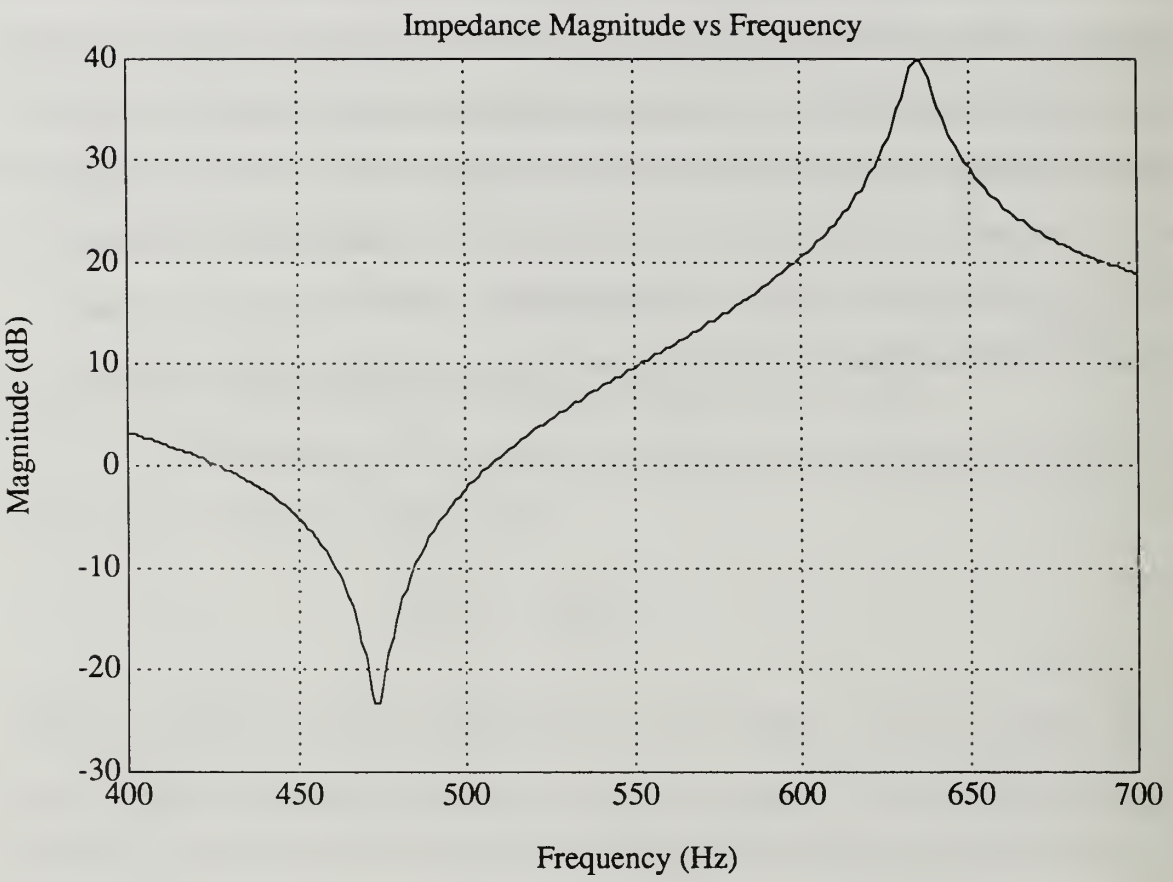
Impedance Magnitude vs Frequency
Magnitude (dB)
40
30
20
10
0
-10
-20
-30
400
450
500
550
600
650
700
Frequency (Hz)

Figure 3.2

IV. MASS ELEMENT RESONATOR TEST

A. EXPERIMENTAL INTENTIONS

This chapter begins with a discussion of the experimental strategy of the mass element resonator test process. This will be followed by an explanation of the experimental setup, and the chapter will finish with the presentation of the results of the data collection. The presentation of intentions and results will be subdivided into sections that address low driver level, or linear, measurements and high driver level, or nonlinear, measurements.

As the title of this thesis states, this paper is intended to characterize the mass element resonator. The strategy formulated to accomplish this characterization was planned so that the response characteristics of the mass element resonator could be explored at both small and large drive level amplitudes. This plan had to be modified somewhat during the course of the mass element testing since unexpected nonlinear responses arose at higher drive levels, but most of the experiment was carried out as intended.

In the first stage of the process, low drive level response data was to be taken. Low drive levels were to be used to insure that the response of the mass element resonator would be linear. Among the low drive level measurements to be taken would be the measurement of the resonant frequency of the mass element resonator at a number of different pressures, effectively changing the value of the gas spring constant, and with different mass loading on the bellows. It was also planned to measure the total resonator losses on resonance and to measure the quality factor, or

Q, of the resonator at the different resonant frequencies. Measurements were also to be taken of the resonance spectrum over a large frequency range.

Following the low drive level measurements, the drive level of the resonator was to be increased to determine how its response changed when it could no longer be considered to be responding linearly. In particular, for the high drive level measurements, it was to be determined whether or not the resonant frequency changed in response to changes in the drive level amplitude. Resonator losses on resonance and Q were also to be examined as they had been for lower drive levels to determine their response to drive amplitude.

Finally, the likelihood of failure of the bellows was not understood. The bellows is a key factor in the resonator, and the lifetime of the bellows is an important variable in determining whether or not the resonator is to have a long service lifetime and low failure rate. Servometer advertises an infinite cycle lifetime for the bellows so long as the operating constraints are not exceeded, but it was felt that these constraints may not be realistic for the use planned for the bellows and that some real measure of operating lifetime was needed. With this in mind, it was planned, upon completion of data collection, to test the bellows to failure to begin to see what sort of lifetime it really had.

This strategy could not anticipate the peculiarities of the bellows' motion that later appeared and needed to be accounted for. It proved, however, to be simple and straight-forward enough that only minor changes were required to explore the nonlinearities when they appeared.

B. EXPERIMENTAL SETUP

With a strategy in hand, the next step was to decide on the parameters to be measured and then to complete the experimental setup. With Hofler's assistance, it was decided that the parameters of interest of the mass element resonator were the pressure and velocity at the driver face. These two parameters could then be combined as a ratio to give a measure of the acoustic impedance of the resonator.

What is desired is the least work being done by the driver for the most acoustic pressure or energy at the stack. The work, W, put into the system by the driver, which is also the power dissipated throughout the acoustic system, P_D, is

$$W = P_D = \frac{1}{2} p_o U_1(x = 0) \tag{4.1}$$

where p_o and U_1 are the pressure and volume velocity, respectively, at the driver (at x = 0). Considering variations at the resonator end of the TAR, keeping the stack and driver the same, then the acoustic energy at the stack is proportional, in the linear regime, to p_o^2. We, therefore, define a figure of merit

$$C = \frac{p_o^2}{W} = \frac{2p_o^2}{p_o U_1(x = 0)} = 2Z_{ac(x = 0)} \tag{4.2}$$

where $Z_{ac(x=0)}$ is the driving point acoustic impedance $p_o/U_{1(x=0)}$. Note that comparison of the various resonators could have been done based on their Q, but this would have been misleading, for although

$$Q = 2\pi \frac{\text{Energy Stored}}{\text{Energy lost per cycle}} = \frac{Kp_o^2}{W} \tag{4.3}$$

where K relates the energy stored to p_o^2, different resonators would have different Ks because different resonator configurations would have energy partitioned differently between the resonator, the stack, and elsewhere.

Data collection for the mass element test was performed using a Hewlett Packard 4192A Impedance Analyzer as the primary measurement instrument. The 4192A is a convenient choice for data collection where the interest is in the acoustic impedance since it will precisely measure the amplitude and phase of the pressure and the velocity signals separately and, more importantly, as a ratio. For amplified, high level signals, ratio errors are typically less than 0.005 dB, and phase errors less than 0.05 degrees. Also, the instrument has a high degree of rejection for noise and harmonic distortion components. While rejection of noise is always good, the rejection of harmonics may cause errors in using the driving point impedance as a figure of merit, as in Equation (4.2). The response of the system at frequencies other than the drive frequency may cause dissipation that is not measured by the 4192A. [Ref. 20]

For the low level measurements, this was negligible as the largest distortion components were always at least -40 dB or lower. For the higher level measurements, some small measurement error may have occurred. The pressure and velocity signal voltages from the acoustic driver are connected to the analyzer inputs B and A respectively, and the 4192A computes the ratio, giving the impedance, in decibels. In this paper, the actual output of the 4192A will most often be referred to as a relative measure of the change in efficiency in the resonator. Comparison of this data for the mass element resonator will also be made to a straight pipe

resonator constructed for the purpose of comparison of acoustic impedances.

The experimental system configuration of the mass element resonator was built on the refrigerator support system that Hofler built for his dissertation refrigerator. In particular, the same microphone and accelerometer were used to supply the pressure signal and, ultimately, the velocity signal inputs to the 4192A through two preamplifiers. The sensitivities of these devices were supplied by Hofler from previous work and were used here in calculations to establish baseline pressure and velocity levels.

Additional equipment used to support the testing of the mass element resonator consisted of a Stanford Research Model SR560 low noise preamplifier for the pressure microphone signal. An Ithaco 1201 low noise preamplifier was used to amplify the accelerometer signal which was sent through an integrator to give a velocity signal output. Both preamplifiers were calibrated prior to use and both demonstrated a good accurate response. The output of both preamplifiers was connected to the 4192A with the pressure signal connected to the B input and the velocity signal connected to the A input.

The experiment also used various subsystems for pressurizing the system and for data collection. Hofler's refrigerator pressurization system allowed the system to be purged and pressurized with helium to provide a pure helium atmosphere in the resonator. Data collected by the HP 4192A impedance analyzer was ported via HPIB to an IBM compatible computer where the data taken during a frequency sweep was written to text files that

were then available for manipulation using various graphing applications or for data extraction.

C. EXPERIMENTAL RESULTS

The first acoustic impedance and Q data looked promising, as did the first few runs over a restricted pressure range. Also the first frequency sweep over a very wide frequency range covering a large region outside the immediate area of the first resonance, Figure 4.1, did not show any cause for concern for nonlinearities. Nice clean response curves similar to the curve plotted for the electrical analogy in Figure 3.2 appeared initially. A more thorough exploration of the pressure range, however, began to reveal the presence of a nonlinear response which grew in extent as the drive levels were increased during subsequent runs. Figure 4.2 shows how the first complete set of frequency sweeps taken for pressures ranging from 15 psig to 135 psig (approximately 2 to 10 bar) looked. The expected resonant peak for the 75 psig frequency sweep near 463 Hz was swallowed up in an unexpected dip in the impedance curve. This first dip was a portent of bigger things to come at higher drive levels.

The relationship of the resonant frequency to the pressure in the resonator is shown in Figure 4.3. It can be seen that the resonant frequency increases with pressure due to the stiffening of the gas springs on either side of the mass element. The Q can also be seen in Figure 4.4 to increase as pressure increases. The Q was determined using two different methods, the first by dividing the resonant frequency by the difference of

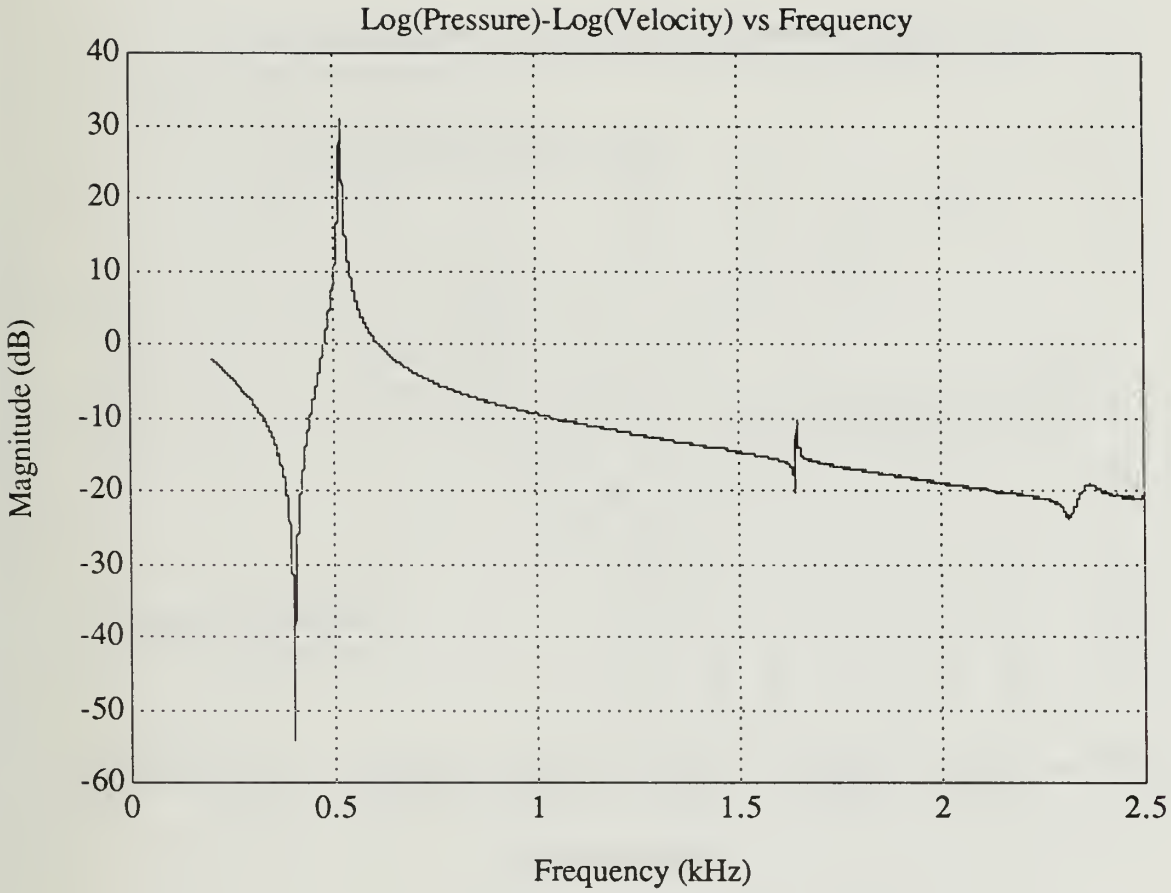
Log(Pressure)-Log(Velocity) vs Frequency
Magnitude (dB)
40
30
20
10
0
-10
-20
-30
-40
-50
-60
0
0.5
1
1.5
2
2.5
Frequency (kHz)

Figure 4.1

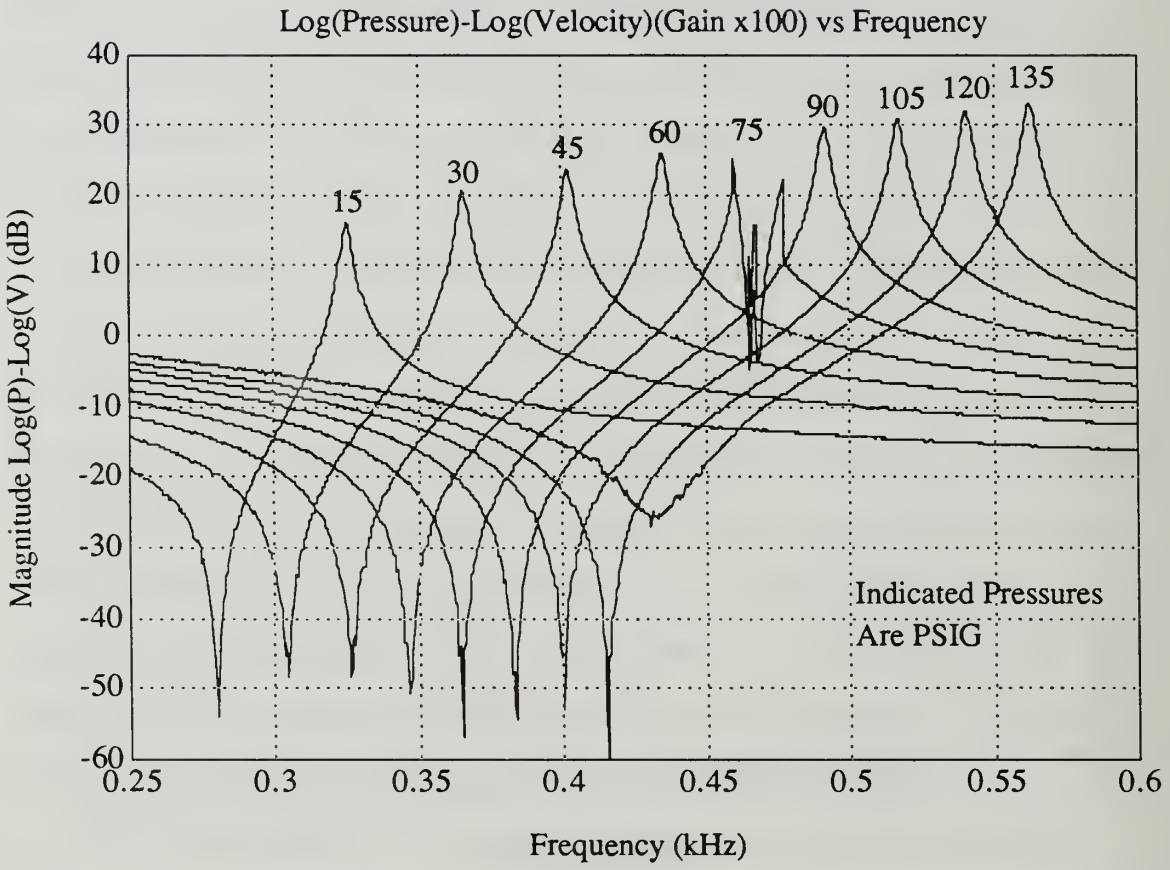
Log(Pressure)-Log(Velocity)(Gain x100) vs Frequency
Magnitude Log(P)-Log(V) (dB)
Frequency (kHz)
40
30
20
10
0
-10
-20
-30
-40
-50
-60
0.25
0.3
0.35
0.4
0.45
0.5
0.55
0.6
15
30
45
60
75
90
105
120
135
Indicated Pressures
Are PSIG

Figure 4.2

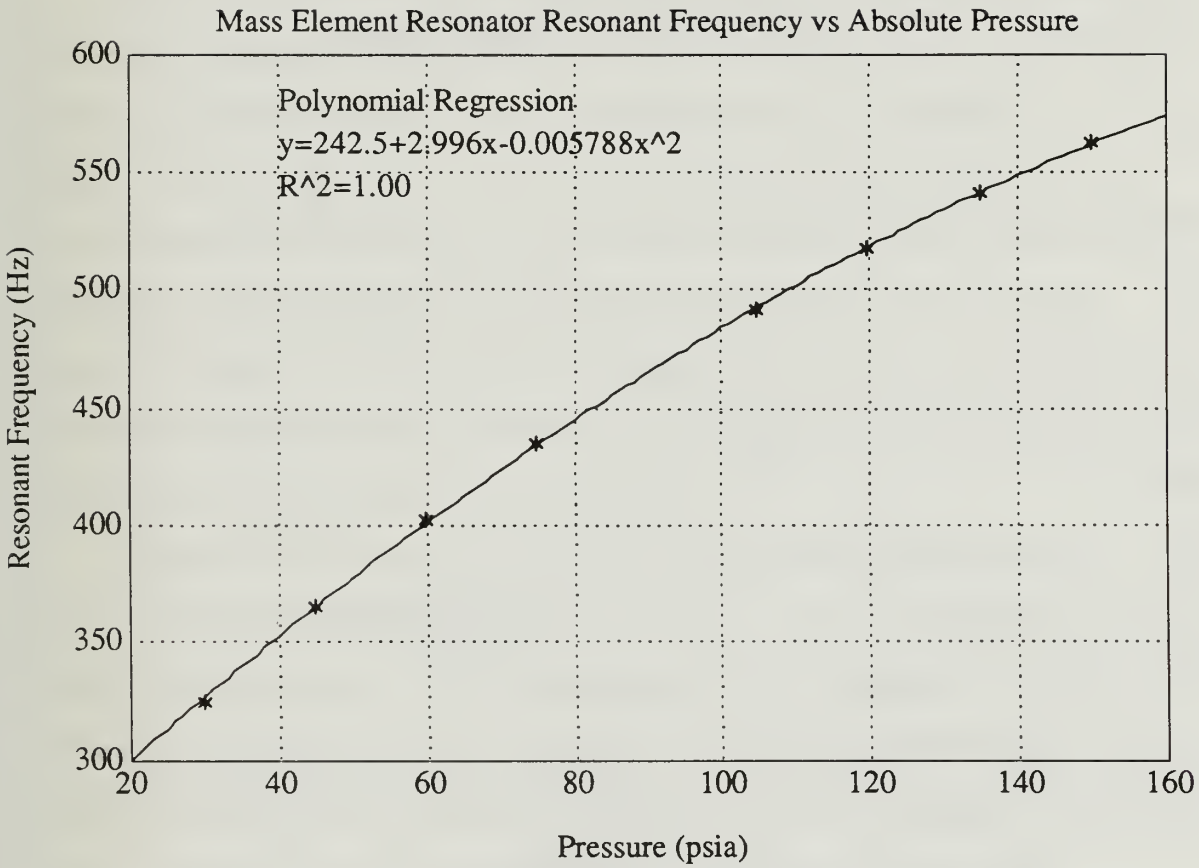
Mass Element Resonator Resonant Frequency vs Absolute Pressure
Polynomial Regression
y=242.5+2.996x-0.005788x^2
R^2=1.00
Resonant Frequency (Hz)
600
550
500
450
400
350
300
20
40
60
80
100
120
140
160
Pressure (psia)

Figure 4.3

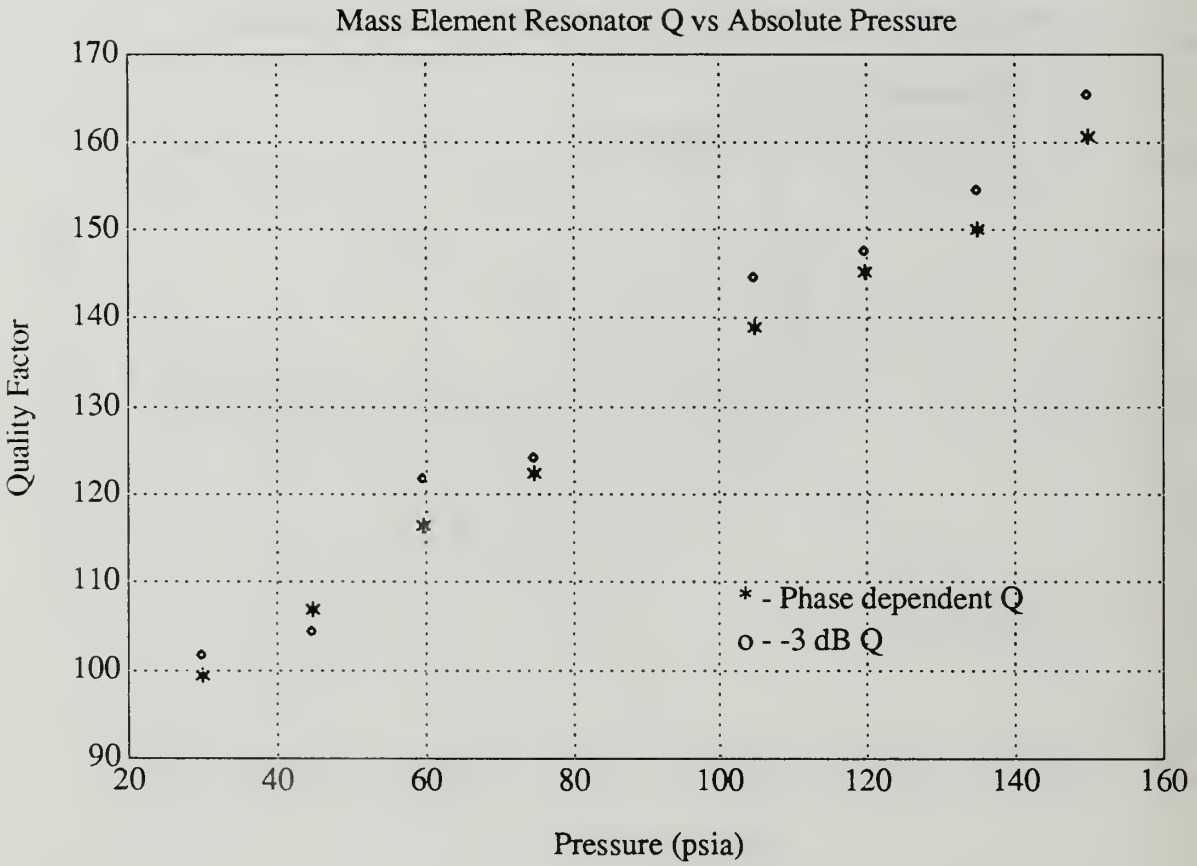
Mass Element Resonator Q vs Absolute Pressure
Quality Factor
Pressure (psia)
170
160
150
140
130
120
110
100
90
20
40
60
80
100
120
140
160
* - Phase dependent Q
o - -3 dB Q

Figure 4.4

the -3 dB frequencies. This compares well with the second method which was devised by Hofler to find Q based on the phase dependence of the pressure and volume velocity near the resonance [Ref. 21]. Figure 4.4 shows the results of both methods for computing Q for the same data.

As was stated earlier, the driving point acoustic impedance provides an alternative measure of the dissipation losses in the resonator, rather than the Q. In order to actually make the comparison of the acoustic impedances and of the Q's, a one-half wavelength straight pipe resonator was constructed and compared to the results obtained with the mass element resonator. The frequency chosen for the comparison was the ten bar resonant frequency of 562.5 Hz. A straight pipe was cut with a length of 0.906 m, a length arrived at by using a sound speed of 1017 m/s for helium at 296 K and several small end corrections.

The pipe was mounted on the same flange that had held the mass element resonator and bolted to the same driver. The pipe was fitted with a pipe cap soldered into place and pressurized with helium to 150 psia. Several frequency sweeps were then done at identical drive levels as had been done with the mass element resonator. Because of minor errors in the actual length of the pipe, the difference in temperature during the experiment compared to that assumed during the calculation of the length, and the difficulty of actually removing all the air from the pipe, the resonant frequency of the pipe was measured to be 558.5 Hz, a difference of 4 Hz or about 0.7 percent from the resonant frequency of the mass element resonator. The calculated resonant frequency of the straight pipe was 560.9 Hz when end corrections and actual cut length of the pipe were

accounted for in the calculations, a difference of less than 0.5 percent from the measured value.

Figure 4.5 shows a comparison of two sweeps, one from the straight pipe, and the other from the mass element resonator. Both were sweeps done at the lowest drive level used during the course of the data collection. The difference in the pressure-velocity ratios at their respective peaks is 9.56 dB, or a factor of 3.01 increase in the ratio for the mass element resonator as compared to the straight pipe. The Q measured for the straight pipe using the half power frequencies is 101. This agrees very well with the theoretical calculation of the Q for a straight pipe which gives a value of 99.5 [Ref. 22]. Compared to the straight pipe, the dissipation losses of the mass element resonator were a factor of 3.01 lower, but because the Q of the mass element resonator (Q=160.5) was only factor of 1.59 higher, the energy stored must be lower by a factor of 1.89. The low level measurements on the mass element resonator were straightforward and presented no particular difficulty. The same cannot be said for the results that were obtained once the drive level was increased to determine the response of the mass element resonator to higher drive levels.
It was thought that the frequency of the resonance might shift with increased drive levels. In fact, the frequency did not shift significantly with drive level. As can be seen in Figure 4.6, the resonant frequency remained within less than 0.2 percent of the value measured during the low level testing. Something else can be seen to be happening, however, that will be addressed in a section to follow on the growing nonlinearities with increased drive levels.

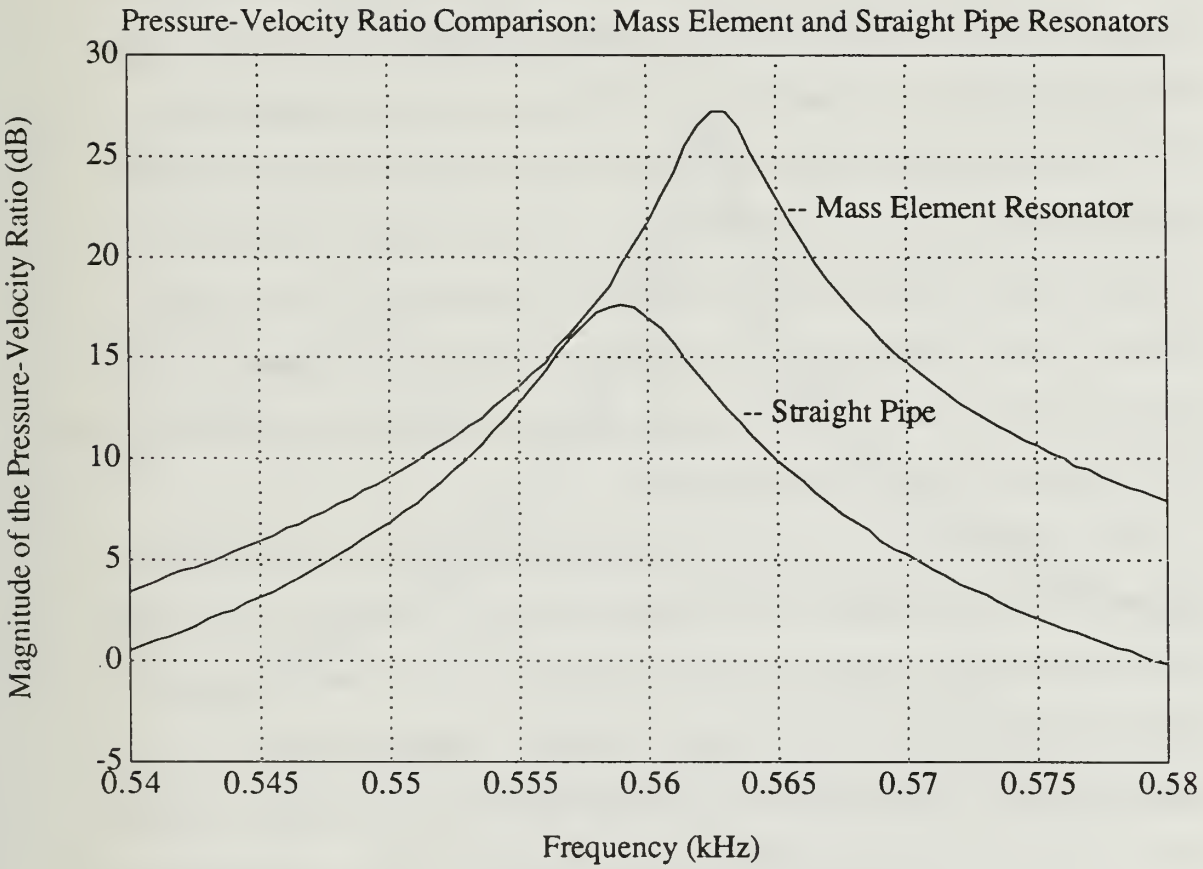
Pressure-Velocity Ratio Comparison: Mass Element and Straight Pipe Resonators
Magnitude of the Pressure-Velocity Ratio (dB)
30
25
20
15
10
5
0
-5
0.54
0.545
0.55
0.555
0.56
0.565
0.57
0.575
0.58
Frequency (kHz)
-- Mass Element Resonator
-- Straight Pipe

Figure 4.5

All the data in Figure 4.6 were taken with the resonator pressurized to 150 psia. The magnitude of the acoustic impedance for these frequency sweeps can be seen to be nearly constant. This means that the dissipation losses remain proportional to the resonator amplitude squared at resonance, an important point, since this probably means that flexural losses in the bellows did not increase dramatically with drive level and that gas losses associated with flow separation and turbulence were not present at a significant level. However, rejection of signal distortion by the 4192A impedance analyzer, may mean that some of the dissipation was not measured, since some of the distortion levels measured at the resonant frequency were substantial. The highest acoustic pressure attained at this point was 0.9 psi peak over the mean pressure in the resonator of 150 psia, or 0.6 percent of mean pressure peak.

The quality factor, Q, was found using the half power frequency method to increase slightly with higher drive levels, ranging from a low near 160 to a high of near 180. One Q measurement taken in this series was not included since it was from a frequency sweep that was compromised by nonlinearities that occurred during the sweep. Overall, the Q appears to have increased about 12.5 percent with a ten-fold increase in drive level, although there is much scatter in the data. Figure 4.7 is a plot of Q against the relative magnitude of the drive level.

For all the things that remained nearly the same during the investigation of the behavior of the mass element resonator, there was some dramatic evidence that things were changing. Figure 4.6 has several

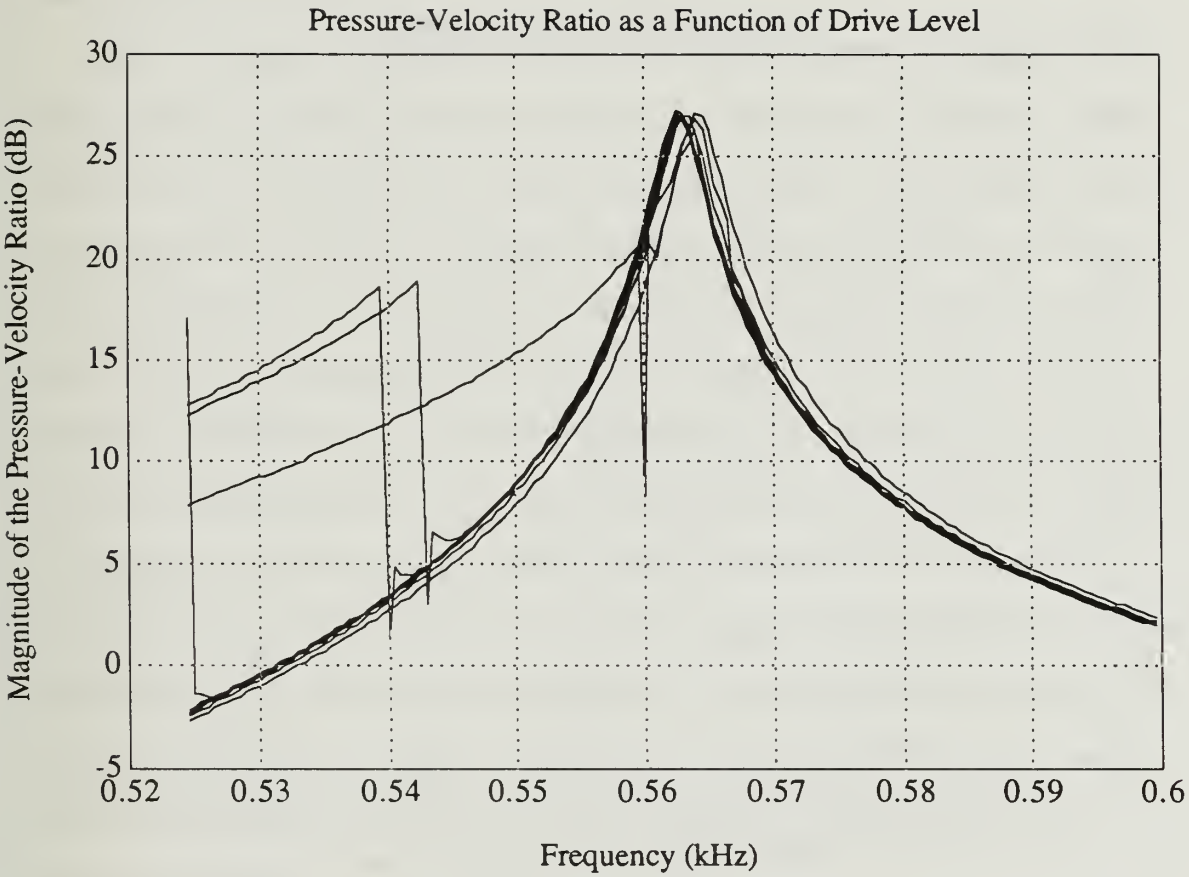
Pressure-Velocity Ratio as a Function of Drive Level
Magnitude of the Pressure-Velocity Ratio (dB)
30
25
20
15
10
5
0
-5
0.52
0.53
0.54
0.55
0.56
0.57
0.58
0.59
0.6
Frequency (kHz)

Figure 4.6

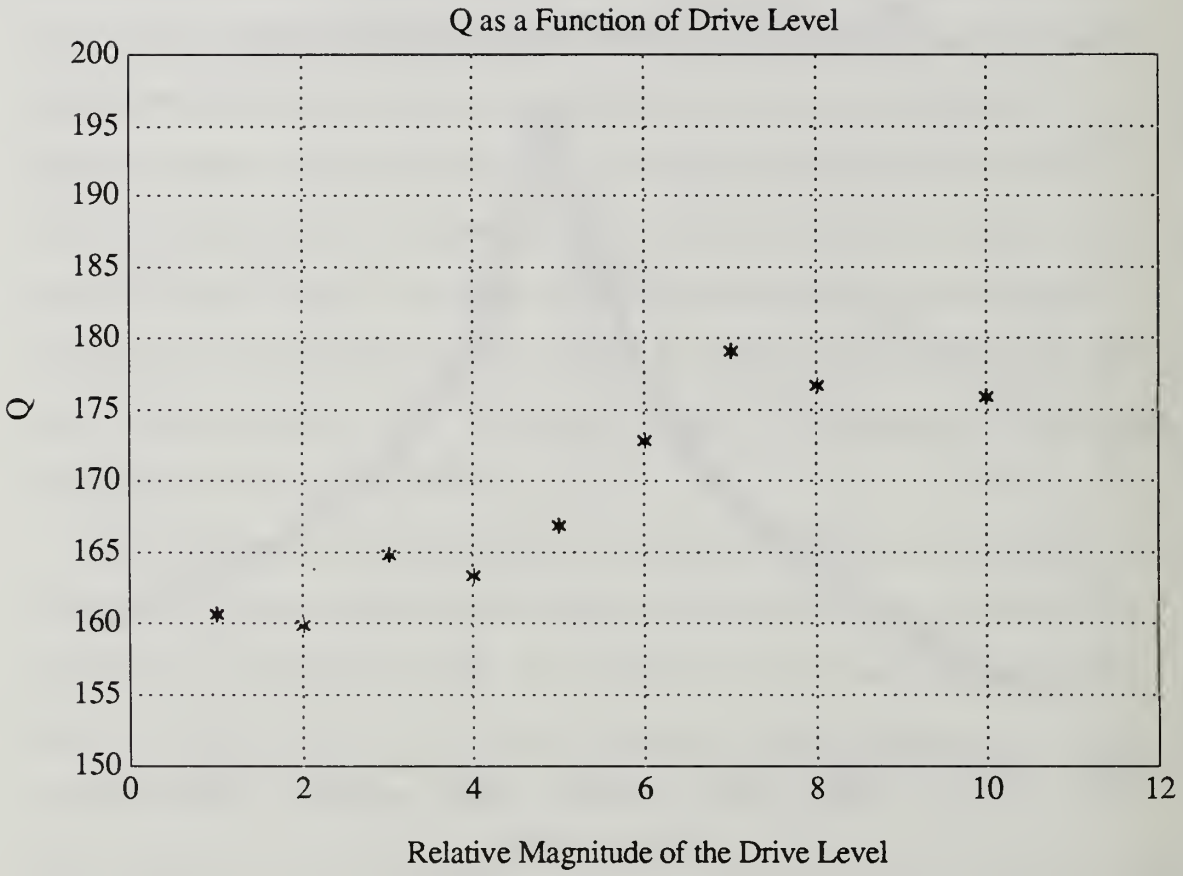
Q as a Function of Drive Level
Q
200
195
190
185
180
175
170
165
160
155
150
0
2
4
6
8
10
12
Relative Magnitude of the Drive Level

Figure 4.7

anomalous lines on the plot. These lines represent the growth of nonlinearities in the response of the mass element resonator with increasing drive level. These nonlinearities become so prominent at the highest levels investigated that they completely overshadow any "normal" response of the mass element resonator.

The anomalies in Figure 4.6 are more clearly shown in Figure 4.8. Here a series of plots have been arranged for comparison. All data were taken at 150 psia and over the same frequency range. Only the drive level was changed for these five frequency sweeps. (The 4192A was used as an input signal source to the driver. In this series of sweeps, the drive levels at the 4192A, measured prior to the driver amplifier were 0.01, 0.03, 0.05,0.07, and 0.09 volts.) The anomaly spreads out in frequency span as the drive level increases. In this plot the resonant peak is still visible but it is engulfed in the anomaly if further increases in drive level are made. The characteristic shape of this curve also changes with the direction of the frequency sweep. The sweeps in Figure 4.8 were made from lower to higher frequencies. In Figure 4.9, a pair of pressure signal sweeps are shown, one taken from lower to higher frequencies, the other in the opposite direction.

The curve shown in Figure 4.9 is known as a bent tuning curve and betrays the presence of hysteresis in the response of the mass element resonator. Curves of this sort gave the first clue of the presence of a nonlinear response from the mass element resonator that had the potential to obscure the desired response. The source of the response that gives rise to the bent tuning curve was not known. In order to obtain another view

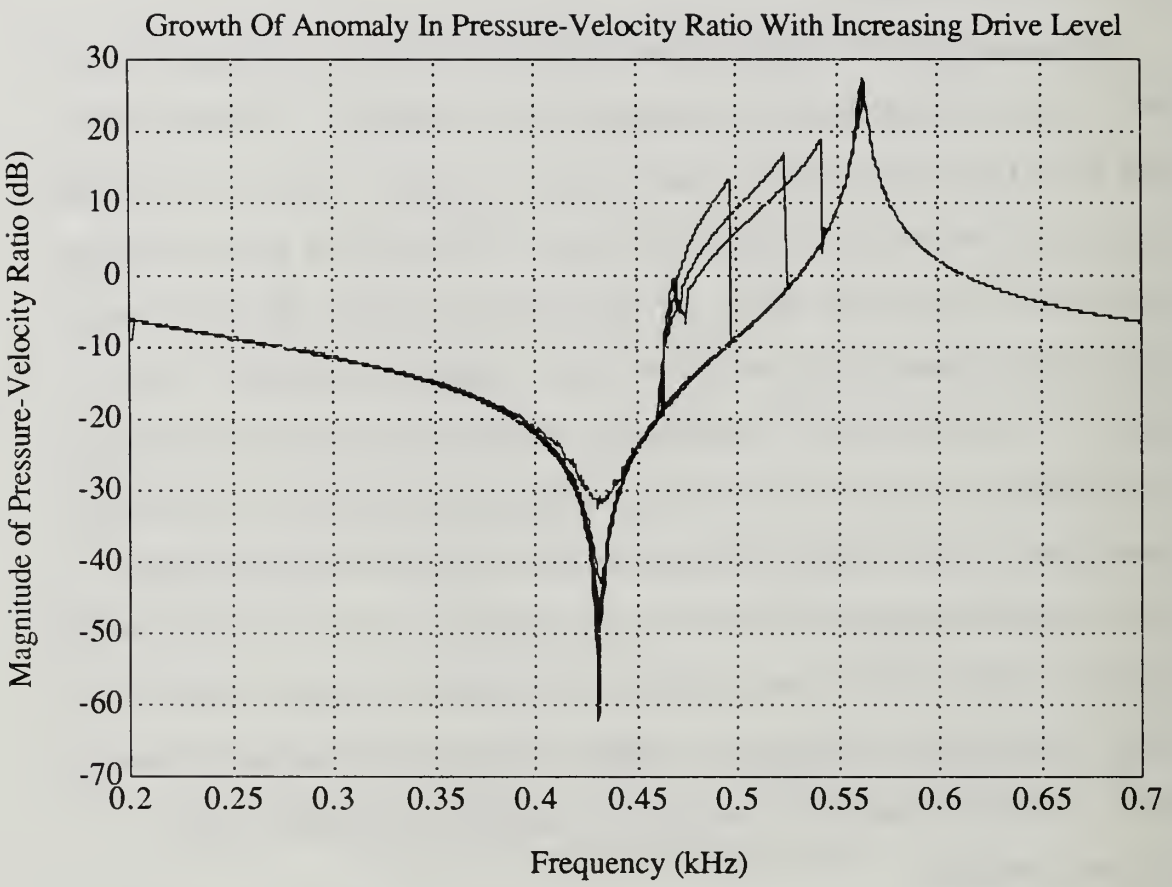
Growth Of Anomaly In Pressure-Velocity Ratio With Increasing Drive Level
Magnitude of Pressure-Velocity Ratio (dB)
30
20
10
0
-10
-20
-30
-40
-50
-60
-70
0.2
0.25
0.3
0.35
0.4
0.45
0.5
0.55
0.6
0.65
0.7
Frequency (kHz)

Figure 4.8

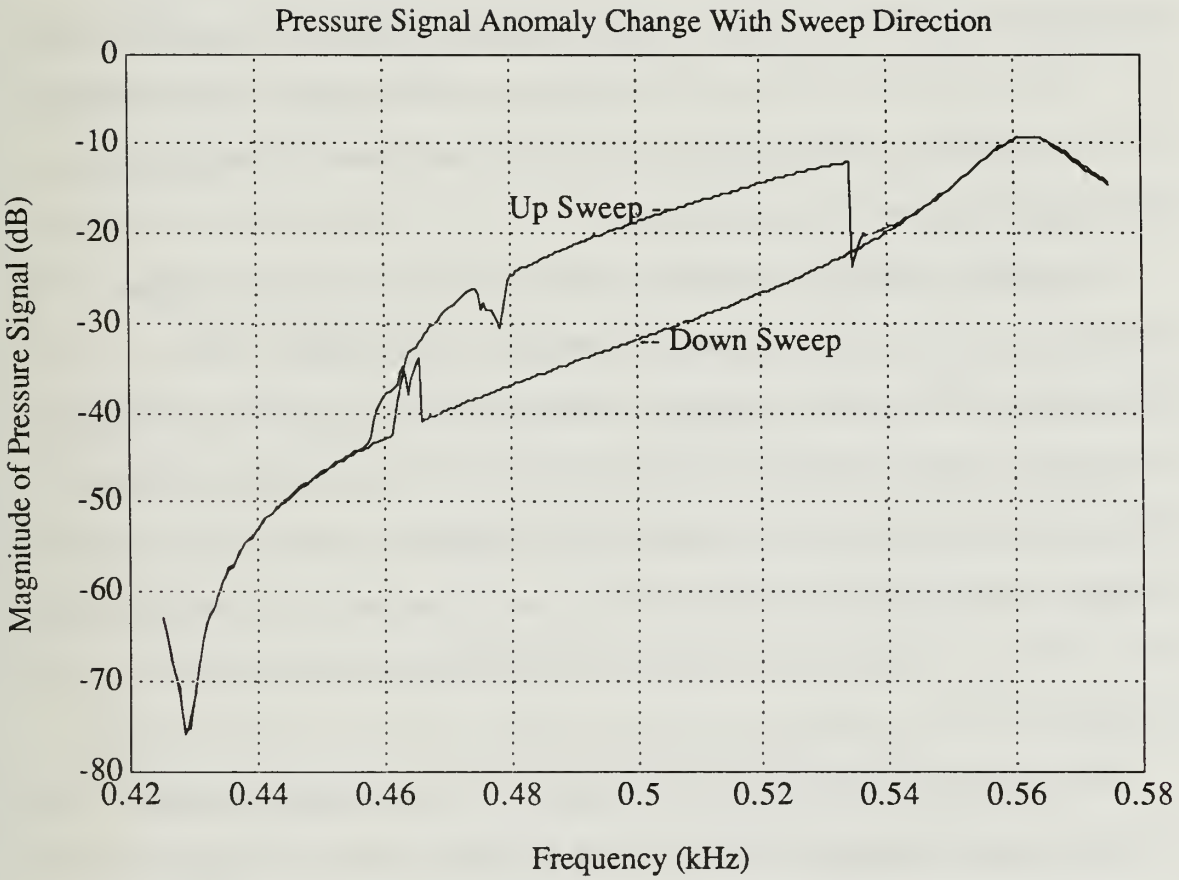
Pressure Signal Anomaly Change With Sweep Direction
Magnitude of Pressure Signal (dB)
0
-10
-20
-30
-40
-50
-60
-70
-80
0.42
0.44
0.46
0.48
0.5
0.52
0.54
0.56
0.58
Frequency (kHz)
Up Sweep
Down Sweep

Figure 4.9

of the problem, in a real sense, it was decided to actually look at the bellows during a frequency sweep.

This proved to be a fortuitous decision. The eye is a marvelous device and when coupled to a strobe light amazing things can be seen. The resonator was depressurized and the end of the resonator covering the bellows was removed, leaving the other end of the resonator attached to the driver. This exposed the face of the bellows so that a strobe light could be shone on the bellows while a frequency sweep was done, allowing the gross motion of the bellows to be observed.

It had been noted previously that whenever the anomalous region appeared in a plot of the pressure or pressure-velocity ratio, that subharmonics of the drive frequency could be observed on the HP3561A. A frequency sweep was started and the bellows observed using the strobe light. At the point where the subharmonics appeared, a new motion was observed from the bellows. The bellows was observed to rock from side to side in addition to displaying a piston motion along the axis of the resonator.

This rocking motion was investigated with the resonator removed from the driver and found to have nearly the same resonant frequency in air as the piston mode. As pressure on the bellows was increased with the pressurization of the resonator, the resonant frequency of the piston mode increased. The rocking mode, however, does not displace gas when it occurs and its resonant frequency does not shift when the resonator is pressurized.

The rocking mode is apparently excited parametrically as the driver sweeps through frequencies that are roughly twice the rocking mode resonant frequency. The fact that the resonator response has a kink and increases sharply at the lower onset frequency in Figure 4.8 and Figure 4.9 also suggests a parametric excitation. The rocking mode resonance lies near 230 Hz and it can be seen from Figure 4.9 that at twice this frequency, 460 Hz, is about where the anomaly appears.

In his dissertation, Keolian includes an appendix on parametrics that was referred to during this portion of the experiment. He calls parametrics one of the most important of a handful of ideas that keep appearing in connection with nonlinear oscillators. Parametrics involves the transfer of energy from one system to another by oscillating a parameter of the second system. What seems to be occurring in the mass element is that energy is in some way being transferred from the piston motion of the bellows into the rocking mode although it is not clear which parameter of the rocking mode is being affected. [Ref.23,24]

What is clear is that the rocking mode can completely obscure the desired piston mode response. A couple of methods were tried with varying success to control the rocking mode without severely affecting the piston mode. The first of these was to insert a steel wool damper into one section of the resonator. The damper was meant to roughly approximate the damping that occurs when there is a stack in place in the resonator. This did not have the desired effect of controlling the rocking mode, however.

The second method to control the rocking does appear to hold out more promise, perhaps in a modified form. In this case, a ring of aluminum was machined to fit the outer radius of the mass that had been previously added to the bellows. Mass was added because this is easier to accomplish than removing mass and because the piston mode frequency was a little higher than was originally intended anyway. It was felt that the addition of this ring lying on the circumference of the bellows would affect the rocking motion more than the piston motion and this indeed proved to be the case. The frequency of the piston mode with the additional mass was lowered about 85 Hz, or 15 percent, and the frequency of the rocking mode was lowered by about 115 Hz, or 25 percent. The response of the mass element at high drive levels was improved, but sufficiently high drive levels were still able to excite the rocking mode. Nevertheless, separating the two modes in frequency space may ultimately prove to be a satisfactory way to control the rocking mode. Figure 4.10 shows two frequency sweeps taken at the same drive level and pressure which show these frequency shifts.

One other method for controlling the rocking of the mass element was also tried. A differential pressure gauge was placed between the two ends of the resonator and a pressure differential was placed across the mass element to place a D.C. bias across the bellows to hopefully find a more linear region for the bellows spring. Figure 4.11 shows the spring rate of the bellows. (Extension is in the positive x direction.)

There is a region when the bellows is slightly compressed that is perhaps more linear, but, as can be seen, only for very small

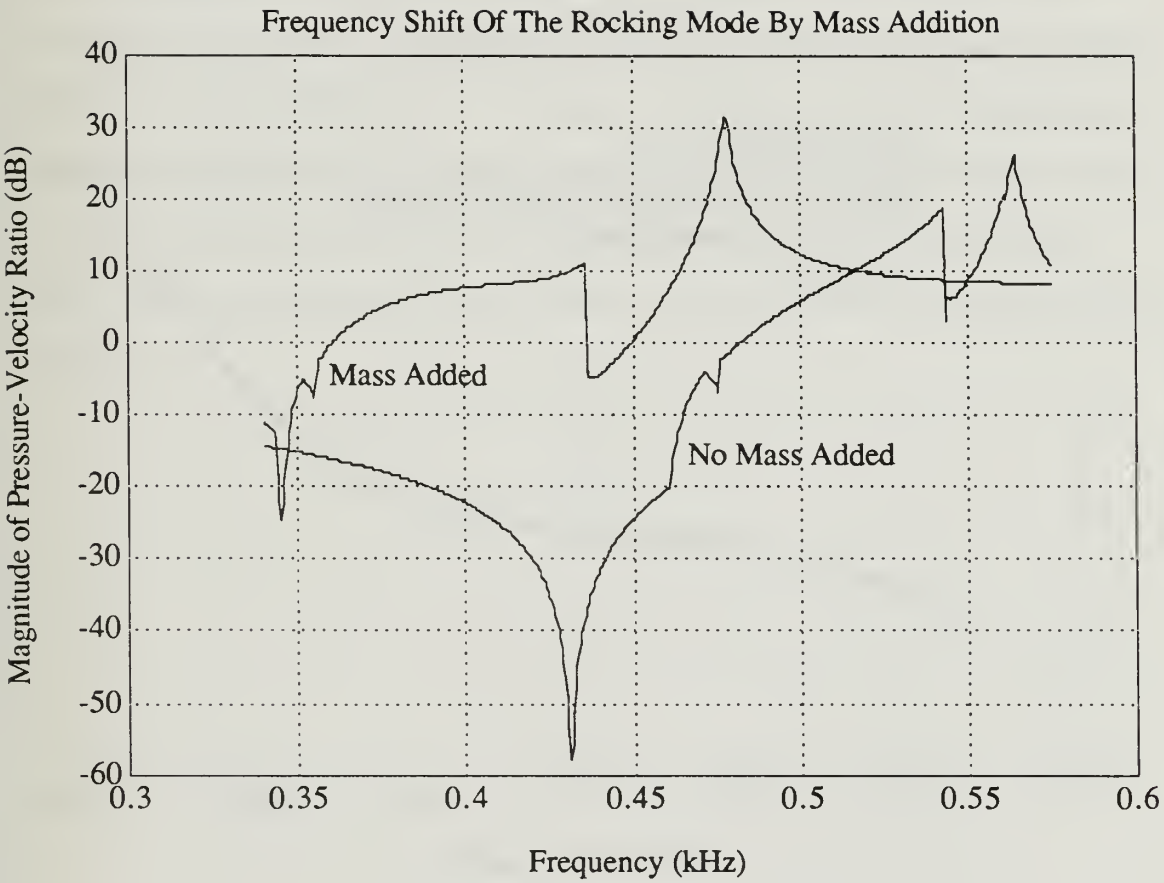
Frequency Shift Of The Rocking Mode By Mass Addition
Magnitude of Pressure-Velocity Ratio (dB)
40
30
20
10
0
-10
-20
-30
-40
-50
-60
0.3
0.35
0.4
0.45
0.5
0.55
0.6
Frequency (kHz)
Mass Added
No Mass Added

Figure 4.10

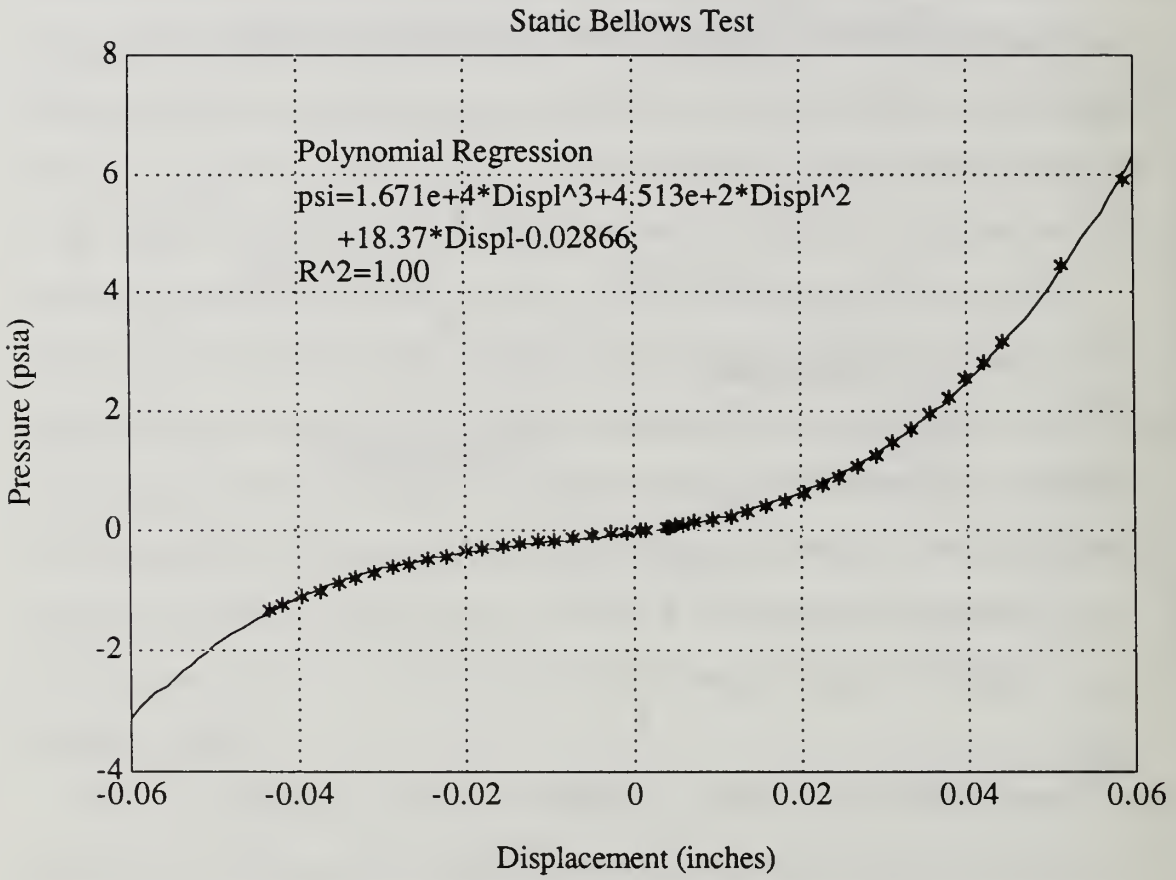
Static Bellows Test
Polynomial Regression
psi=1.671e+4*Displ^3+4.513e+2*Displ^2
+18.37*Displ-0.02866;
R^2=1.00
Pressure (psia)
Displacement (inches)
8
6
4
2
0
-2
-4
-0.06
-0.04
-0.02
0
0.02
0.04
0.06

Figure 4.11

displacements. Because the bellows' spring rate is so nonlinear this attempt to find a linear region for operating the bellows was not successful. An early sweep with the bellows held in compression seemed indicate some improvement in the response but this could not be duplicated on subsequent sweeps, leading to the conclusion that the response of the bellows was improved very little by holding it in compression during frequency sweeps and not at all by holding it in extension. The only one of the methods that appears at this point to hold any promise of controlling the rocking mode is a method that relies on changing the moment of inertia of the rocking mode. Plans are presently being made to try to do this in a subsequent test resonator.

V. CONCLUSIONS AND RECOMMENDATIONS

This thesis has attempted to describe a modification undertaken in order to build a more efficient resonator for a cryocooler version of the Thermoacoustic Refrigerator. The substitution of a solid mass-spring element as an impedance matched replacement for a section of the gas-filled resonator tube and, in particular, the use of a Servometer electroformed single convolution nickel bellows, has been explored. It is apparent that the bellows selected had modes of response that were not anticipated. The discovery of this sort of information is, of course, one of the primary reasons for doing experimental research.

The mass element modification to the resonator appears to be a promising way in which the efficiency of the resonator can be increased but this will depend on the ability to control the rocking mode that interferes with the desired piston mode. The appearance of the nonlinearities in the vibration of the bellows requires modifications to control the undesirable motions of the bellows in order to make it conform to the motion of a planar piston resonating at the same frequency and with the same impedance as the section of replaced resonator pipe.

Early attempts to control the rocking motion suggest that increasing the moment of inertia of the rocking mode may allow the rocking mode to be suppressed or displaced in frequency sufficiently to prevent its interference with the piston mode. The planned use of one or possibly two 2.25 in. bellows in the next test resonator may eliminate the need to go to any great lengths in this direction since it is not clear just which

characteristics of the 1.5 in. bellows will be shared with its larger brother. One other suggestion for future testing which has been discussed is a plan to instrument the next bellows-mass element so that its motion can be observed in a more quantitative manner that was permissible with the eye-strobe light combination.

REFERENCES

1. Strutt, John W., Lord Rayleigh, *The Theory of Sound*, 2d ed., v.2, pp. 230-231, MacMillan and Co., Ltd., 1929.

2. Wheatley, J., Hofler,T., Swift, G.W., and Migliori, A., "Understanding some simple phenomena in thermoacoustics with applications to acoustical heat engines," *American Journal of Physics*, v. 53, No. 2, pp. 148, February 1985. The authors cite a number of articles by Wheatley, Angew, Müller, and Zouzoulas that develop the quantitative approach to the problem.

3. Hofler, T.J., *Thermoacoustic Refrigeration Design and Performance*, Ph.D. Dissertation, University of California, San Diego, California, 1986.

4. Harris, David A., and Volkert, Richard E., *Design and Calibration of an Electrodynamic Driver for the Space Thermoacoustic Refrigerator*, Master's Thesis, Naval Postgraduate School, Monterey, California, December 1989.

5. Byrnes, R. B., *Electronics for Autonomous Measurement and Control of a Thermoacoustic Refrigerator in a Space Environment*, Master's Thesis, Naval Postgraduate School, Monterey, June 1989.

6. Susalla, M. P., *Thermodynamic Improvements for the Space Thermoacoustic Refrigerator (STAR)*, Master's Thesis, Naval Postgraduate School, Monterey, California, June 1988.

7. Fitzpatrick, Michele, *Electrodynamic Driver for the Space Thermoacoustic Refrigerator (STAR)*, Master's Thesis, Naval Postgraduate School, Monterey, California, March 1988.

8. Adeff, Jay A., *Measurement of the Space Thermoacoustic Refrigerator Performance*, Master's Thesis, Naval Postgraduate School, Monterey, California, September 1990.

9. Harris and Volkert, pp. 26-27.

10. Adeff, pp. 75-83.

11. Adeff, pp. 70-75.

12. Wheatley, J., Hofler,T., Swift, G.W., and Migliori, A., "An Intrinsically Irreversible Thermoacoustic Heat Engine," *JASA*, v. 74, No. 1, pp. 153, July 1983.

13. Wheatley, John, and Cox, Arthur, "Natural Engines," *Physics Today*, August 1985.

14. Wheatley and Cox, pp. 52.

15. Hofler, dissertation, pp 11-12.

16. Hofler, dissertation, pp 12.

17. Kinsler, John W., Frey, A. R., Coppens, A. B., Sanders, J. V., *Fundamentals of Acoustics,* 3d ed., pp. 203, John Wiley & Sons, 1982.

18. Hofler, dissertation, pp 15-23.

19. Kinsler, pp 200-202, and 210-214.

20. Hewlett Packard, *Model 4192A LF Impedance Analyzer, Operation and Service Manual*, pp 1-1, Yokogawa-Hewlett-Packard, LTD., 1984.

21. Hofler, "Accurate ...", pp. 784.

22. Swift, G.W., "Thermoacoustic Engines," *JASA*, v. 84, No. 4, pp. 1163, October, 1988

23. Keolian, R.M., *Modulations of Driven Nonlinear Surface Waves on Water and Liquid Helium-4*, Ph.D. Dissertation, University of California, Los Angeles, California, 1985.

24. Pippard, A. B., *The Physics of Vibration*, Omnibus ed., Cambridge University Press, 1989.

INITIAL DISTRIBUTION LIST

		No. Copies
1.	Defense Technical Information Center Cameron Station Alexandria, Virginia 22304-6145	2
2.	Library, Code 52 Naval Postgraduate School Monterey, California 93943-5100	2
3.	Dr. T Hofler, Code PH/HF Naval Postgraduate School Monterey, California 93943-5100	5
4.	Professor S. L. Garrett, Code PH/GX Naval Postgraduate School Monterey, California 93943-5100	1
5.	Professor R. Keolian, Code PH/K Naval Postgraduate School Monterey, California 93943-5100	1
6.	Jay Adeff, Code PH/AF Naval Postgraduate School Monterey, California 93943-5100	1
7.	Lt. Larry A. Grant 246 Worden Street Portsmouth, RI 02871	2
8.	Eric Moore, Code PH/MR Naval Postgraduate School Monterey, California 93943-5100	1